"Study of the Cold Dense Baryonic Matter with Nonpolarized and Polarized Beams"

S.S. Shimanskiy (VBLHEP JINR, Dubna)

Plan

1. Cold Quark-Gluon Phase (Region of Quark Dominance)
2. Cumulative (and subthreshold) processes
3. DINR at high p_T as probes of the cold dense nuclear matter
4. Which high p_T problems for spin are interesting in our energy range?
5. p_T~2 GeV/c anomaly
6. What "new" we can propose?
7. How its can be done?

Cold Quark-Gluon Phase

(Region of Quark Dominance)

RHIC Physics: 3 Lectures*

Larry McLerran
Physics Department PO Box 5000 Brookhaven National Laboratory Upton, NY 11973 USA

September 13, 2003

+ CERN Yellow Report 2007-005, p.75 2008-005

The Evolving QCD Phase Transition

t ~ 1980

T

Quark Gluon Plasma

Hadron Gas

μ_B

Critical Temperature 150 - 200 MeV ($\mu_B = 0$)

Critical Density 1/2-2 Baryons/Fm^3 (T = 0)

Nuclear Physics A 837 (2010) 65-86

Nuclotron-SPS Time (CERN)

RHIC Time(BNL)

t ~ 1990

T

Quark Gluon Plasma

Hadron Gas

μ_B

t ~ 2000

T

Quark Gluon Plasma

Color Superconducto

Hadron Gas

μ_B

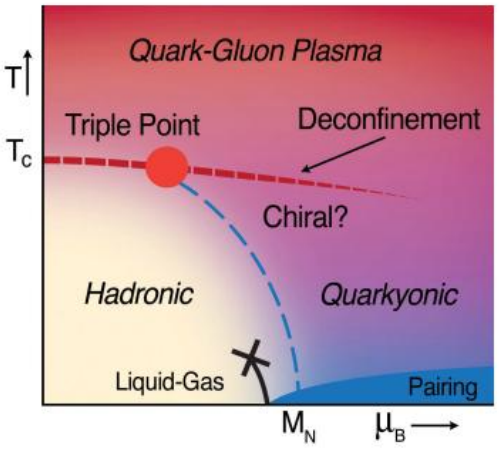

Figure 4: A phase diagram for QCD collisions.

astro-ph/0604422 v1 20 Apr 2006

FRIDOLIN WEBER,* ALEXANDER HO,† RODRIGO P. NEGREIROS,‡
PHILIP ROSENFIELD§

$H \sim 10^{17}$ Gs !

$E \sim 10^{19}$ V/cm

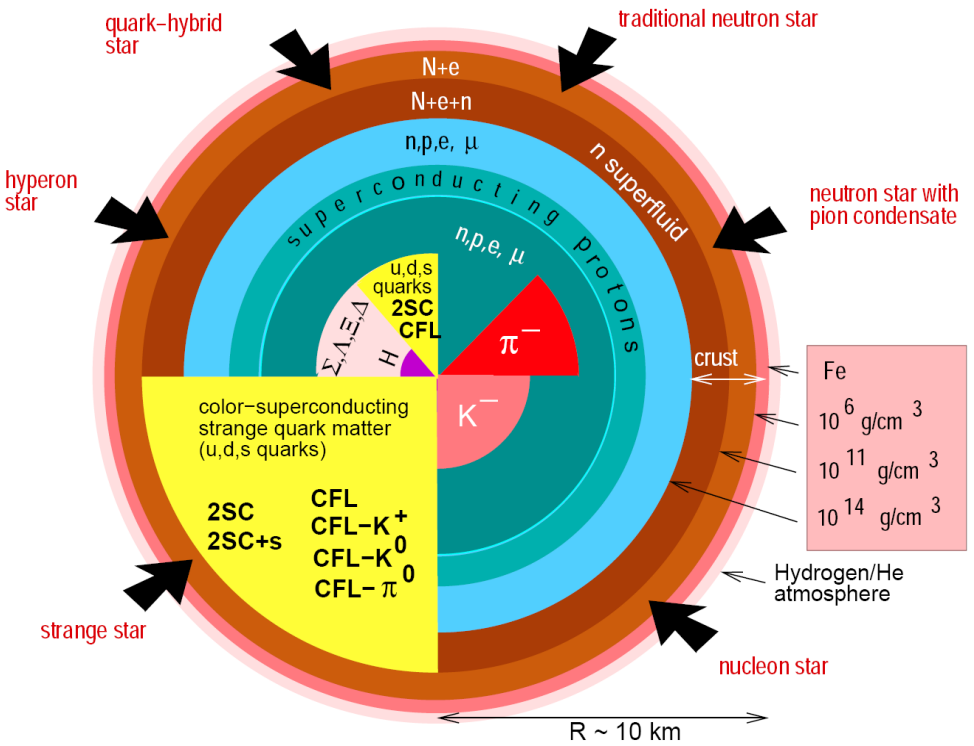

Fig. 1. Competing structures and novel phases of subatomic matter predicted by theory to make their appearances in the cores ($R \lesssim 8$ km) of neutron stars[4].

significant range of chemical potentials and strange quark masses[51]. If the strange quark mass is heavy enough to be ignored, then up and down quarks may pair in the two-flavor superconducting (2SC) phase. Other possible condensation patters

color–superconducting strange quark matter (u,d,s quarks)

K. Rajagopal and F. Wilczek, *The Condensed Matter Physics of QCD*, At the Frontier of Particle Physics / Handbook of QCD, ed. M. Shifman, (World Scientific) (2001).
M. Alford, Ann. Rev. Nucl. Part. Sci. **51** (2001) 131.

Cumulative (and subthreshold) processes

High p_T processes, Cumulative and Subthreshold particle productions are very nice tools to investigate the high dense state of the cold nuclear matter.

Back to Rutherford (high transfers processes)

Hard Hadron - Nucleus Processes And Multi - Quark Configurations In Nuclei.
A.V. Efremov, V.T. Kim, G.I. Lykasov, (Dubna, JINR) . JINR-E2-85-537, Jul 1985. 14pp.
Published in Sov.J.Nucl.Phys.44:151,1986, Yad.Fiz.44:241-249,1986

1. Distributions in nuclei and in free nucleons are different due to the Fermi-motion of nucleons and a possible presence of the multiquark fluctons /1-3/;

2. Hard hadron-nucleus interaction can be more complicated in contrast with the deep inelastic lepton-nucleon scattering because of the multiple rescattering effects of quarks of a colliding hadron and the absorption of secondary hadrons /10/.

V. Conclusion

The analysis of the inclusive large x_1 meson production in the hard hadron processes on nuclei has allowed one to understand the relative contribution of multiple rescattering processes and the existence of multiquark fluctons in the nucleus in dependence on x_1 the multiple rescattering processes are dominating at $x_1 < 0.7 \div 0.8$ whereas at larger x_1 the mechanism of hard scattering on fluctons is dominating. The model of multiple rescattering in which the multiple soft collisions suggested in this paper are taken into account before the hard collision allows one to describe the multiple rescattering processes inside the nucleus correctly.

The fluctons model succesfully used earlier for the description of the cumulative production and EMC-effect with such parameters is applied for the description of anomalous phenomena in the large p_1 processes in nuclei.

DIS at $x > 1$

K.Rith From Nuclei to Nucleons (Summary)

Nuclear Physics A532 (1991) 3c-14c

2.6. Region 5

In the region $x > 1$ the struck quark is 'superfast', its momentum is larger than the momentum allowed for a stationary nucleon. The longitudinal distances involved are $z < 0.2$ fm and therefore one is sensitive to correlations of nearby nucleons or more complicated configurations like multiquark clusters. As an example the predictions for a multiquark cluster calculation [32] are shown in figure 5.

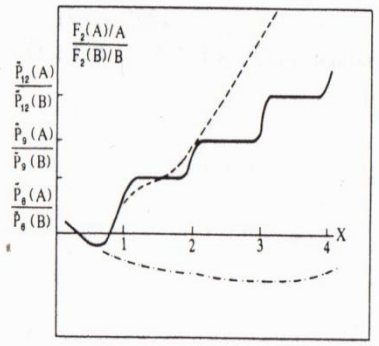

Figure 5. Theoretical predictions for nuclear structure functions at $x > 1$

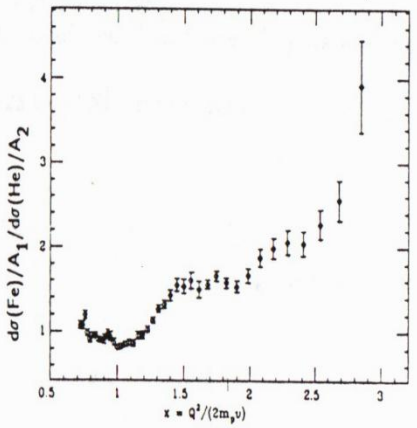

Figure 6. Preliminary results for σ^{Fe}/σ^{He} from NE-2 at SLAC

The height of the plateau in the range $1 < x < 2$ is proportional to the ratio of probabilities of finding 6-quark clusters in nuclei A and B, the range $2 < x < 3$ reflects the ratio of 9-quark cluster probabilities and so on.

Figure 6 shows preliminary results for the cross section ratio of Fe and He obtained by NE-2 at SLAC [33], which took data for a series of nuclei with beam energies between 4 and 14 GeV. One could speculate that the plateau for $1.5 < x < 2$ is an indication for the step function expected in the multiquark cluster model. Note, however, that the data are still substantially affected by quasielastic scattering as the ratio is smaller than one near $x = 1$.

32 J. Vary, Proceedings of the 7th Int. Conf. on High Energy Physics problems, Dubna 1984,147.

PHYSICAL REVIEW C VOLUME 45, NUMBER 4 APRIL 1992

Nuclear structure functions at $x > 1$

B. W. Filippone, R. D. McKeown, R. G. Milner,* and D. H. Potterveld†
Kellogg Radiation Laboratory, California Institute of Technology, Pasadena, California 91125

D. B. Day, J. S. McCarthy, Z. Meziani,‡ R. Minehardt, R. Sealock, and S. T. Thornton
Institute of Nuclear and Particle Physics and Department of Physics, University of Virginia, Charlottesville, Virginia 22901

J. Jourdan and I. Sick
Institut für Physik, Universität Basel, CH-4056, Basel, Switzerland

Z. Szalata
American University, Washington, D.C. 20016
(Received 19 April 1991)

Nuclear structure functions are extracted for high-energy electron scattering from nuclei at large values of the kinematic variable x and Q^2 in the range 1–4 $(\mathrm{GeV}/c)^2$. At the highest Q^2, the data for $x > 1$ begin to display a scaling indicative of local duality.

PACS number(s): 25.30.Fj, 13.60.Hb

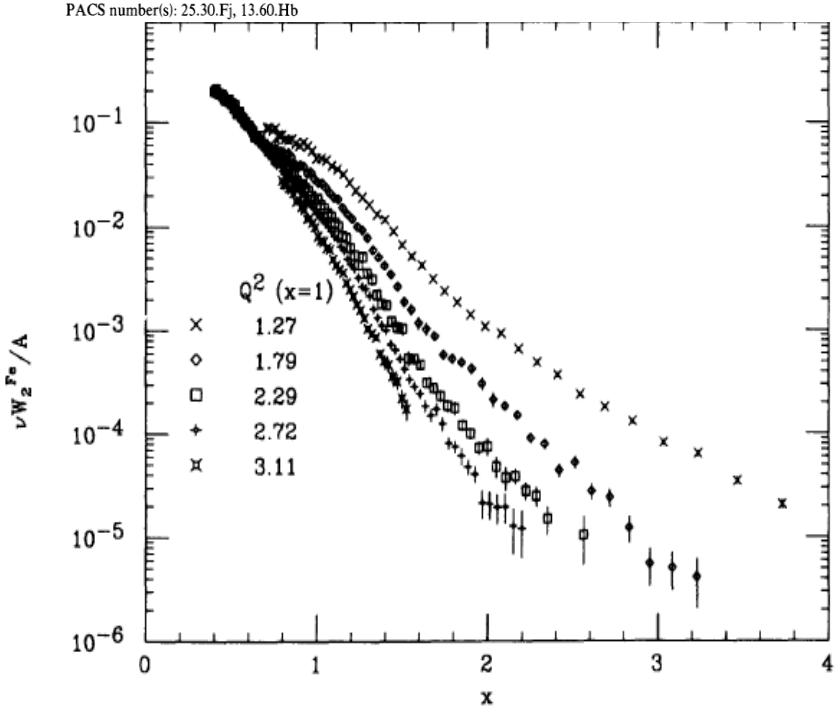

FIG. 1. Measured structure function per nucleon for Fe vs x. The Q^2 value at $x = 1$ is also listed for the different kinematics.

To check this idea SLAC existing data were reanalyzed

- The old SLAC data were analyzed
  - A/D ratios were extracted for A=4,12, 27, 56
  - Evidence for scaling is obvious
  - Scaling factors were used to estimate 2-nucleon **SRC** probabilities in nuclei A relative to D

Frankfurt,Strikman,Day, Sargsian, Phys.Rev. C '93

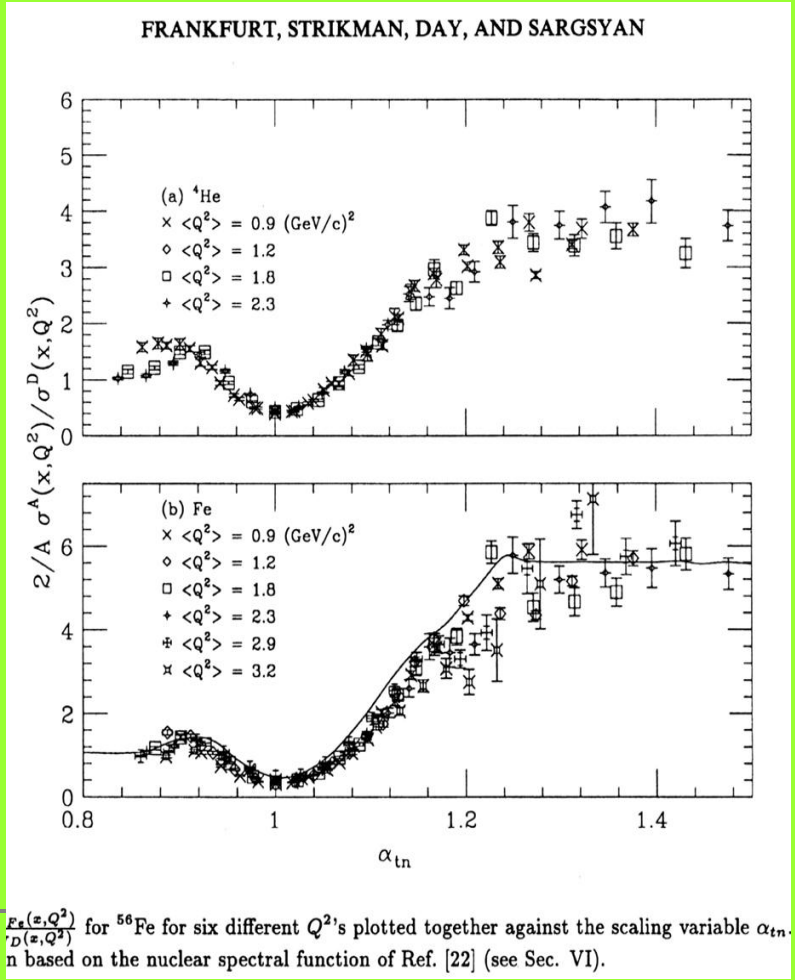

$\frac{F_e(x,Q^2)}{F_D(x,Q^2)}$ for ^{56}Fe for six different Q^2's plotted together against the scaling variable α_{tn}. n based on the nuclear spectral function of Ref. [22] (see Sec. VI).

However

- Data for nuclei A and for D were measured in large difference of kinematics, the theoretical calculation were used to obtain data at the same Q^2 and x_B for heavy nuclei and D
- Absolute probabilities were no able to obtain
- x_B interval used was limited (<1.6)
- **Systematic and dedicated measurements are needed**

Z. Phys. C 63, 29–36 (1994)

ZEITSCHRIFT
FÜR PHYSIK C

Nuclear structure functions in carbon near $x = 1$

BCDMS Collaboration

Abstract. Data from deep inelastic scattering of 200 GeV muons on a carbon target with squared four-momentum transfer $52\,\mathrm{GeV}^2 \leq Q^2 \leq 200\ \mathrm{GeV}^2$ were analysed in the region of the Bjorken variable close to $x = 1$, which is the kinematic limit for scattering on a free nucleon. At this value of x, the carbon structure function is found to be $F_2^C \approx 1.2 \cdot 10^{-4}$. The x dependence of the structure function for $x > 0.8$ is well described by an exponential $F_2^C \propto \exp(-sx)$ with $s = 16.5 \pm 0.6$.

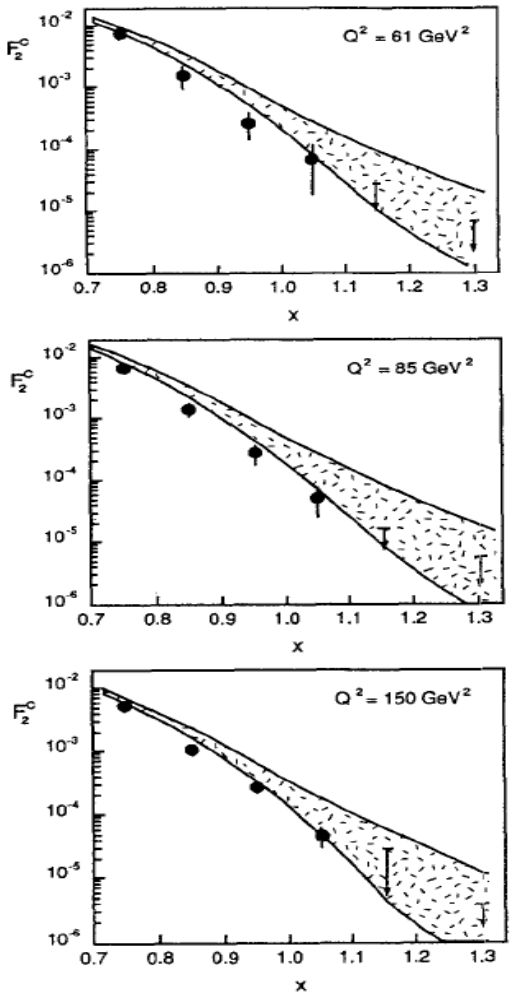

Fig. 7. The nuclear structure function $F_2^C(x)$ as a function of x, at three different values of Q^2. The hatched regions show the range of predictions of [26]

PHYSICAL REVIEW C **68**, 014313 (2003)

Observation of nuclear scaling in the $A(e,e')$ reaction at $x_B>1$

PRL **96**, 082501 (2006) PHYSICAL REVIEW LETTERS week ending 3 MARCH 2006

Measurement of Two- and Three-Nucleon Short-Range Correlation Probabilities in Nuclei

K. S. Egiyan,[1,34] N. B. Dashyan,[1] M. M. Sargsian,[10] M. I. Strikman,[28] L. B. Weinstein,[27] G. Adams,[30] P. Ambrozewicz,[10] M. Anghinolfi,[16] B. Asavapibhop,[22] G. Asryan,[1] H. Avakian,[34] H. Baghdasaryan,[27] N. Baillie,[38] J. P. Ball,[2] N. A. Baltzell,[33] V. Batourine,[20] M. Battaglieri,[16] I. Bedlinskiy,[18] M. Bektasoglu,[27] M. Bellis,[30,4] N. Benmouna,[12] A. S. Biselli,[30,4] B. E. Bonner,[31] S. Bouchigny,[34,17] S. Boiarinov,[34] R. Bradford,[4] D. Branford,[9] W. K. Brooks,[34] S. Bültmann,[27] V. D. Burkert,[34] C. Bultuceanu,[38] J. R. Calarco,[24] S. L. Careccia,[27] D. S. Carman,[26] B. Carnahan,[5] S. Chen,[11] P. L. Cole,[34,14] P. Coltharp,[11,34] P. Corvisiero,[16] D. Crabb,[37] H. Crannell,[5] J. P. Cummings,[30] E. De Sanctis,[15] R. DeVita,[16] P. V. Degtyarenko,[34] H. Denizli,[29] L. Dennis,[11] K. V. Dharmawardane,[27] C. Djalali,[33] G. E. Dodge,[27] J. Donnelly,[13] D. Doughty,[7,34] P. Dragovitsch,[11] M. Dugger,[2] S. Dytman,[29] O. P. Dzyubak,[33] H. Egiyan,[24] L. Elouadrhiri,[34] A. Empl,[30] P. Eugenio,[11] R. Fatemi,[37] G. Fedotov,[23] R. J. Feuerbach,[4] T. A. Forest,[27] H. Funsten,[38] G. Gavalian,[27] N. G. Gevorgyan,[1] G. P. Gilfoyle,[32] K. L. Giovanetti,[19] F. X. Girod,[6] J. T. Goetz,[3] E. Golovatch,[16] R. W. Gothe,[33] K. A. Griffioen,[38] M. Guidal,[17] M. Guillo,[33] N. Guler,[27] L. Guo,[34] V. Gyurjyan,[34] C. Hadjidakis,[17] J. Hardie,[7,34] F. W. Hersman,[24] K. Hicks,[26] I. Hleiqawi,[26] M. Holtrop,[24] J. Hu,[30] M. Huertas,[33] C. E. Hyde-Wright,[27] Y. Ilieva,[12] D. G. Ireland,[13] B. S. Ishkhanov,[23] M. M. Ito,[34] D. Jenkins,[36] H. S. Jo,[17] K. Joo,[37,8] H. G. Juengst,[12] J. D. Kellie,[13] M. Khandaker,[25] K. Y. Kim,[29] K. Kim,[20] W. Kim,[27,20] A. Klein,[27,20] F. J. Klein,[27] A. Klimenko,[27] M. Klusman,[30] L. H. Kramer,[10,34] V. Kubarovsky,[30] J. Kuhn,[4] S. E. Kuhn,[27] S. Kuleshov,[18] J. Lachniet,[4] J. M. Laget,[6,34] J. Langheinrich,[33] D. Lawrence,[22] T. Lee,[24] K. Livingston,[13] L. C. Maximon,[12] S. McAleer,[11] B. McKinnon,[13] J. W. C. McNabb,[4] B. A. Mecking,[34] M. D. Mestayer,[34] C. A. Meyer,[4] T. Mibe,[26] K. Mikhailov,[18] R. Minehart,[37] M. Mirazita,[15] R. Miskimen,[22] V. Mokeev,[23,34] S. A. Morrow,[6,17] J. Mueller,[29] G. S. Mutchler,[31] P. Nadel-Turonski,[12] J. Napolitano,[30] R. Nasseripour,[10] S. Niccolai,[12,17] G. Niculescu,[26,19] I. Niculescu,[12,19] B. B. Niczyporuk,[34] R. A. Niyazov,[34] G. V. O'Rielly,[22] M. Osipenko,[16,23] A. I. Ostrovidov,[11] K. Park,[20] E. Pasyuk,[2] C. Peterson,[13] J. Pierce,[37] N. Pivnyuk,[18] D. Pocanic,[37] O. Pogorelko,[18] E. Polli,[15] S. Pozdniakov,[18] B. M. Preedom,[33] J. W. Price,[3] Y. Prok,[34] D. Protopopescu,[13] L. M. Qin,[27] B. A. Raue,[10,34] G. Riccardi,[11] G. Ricco,[16] M. Ripani,[16] B. G. Ritchie,[2] F. Ronchetti,[15] G. Rosner,[13] P. Rossi,[15] D. Rowntree,[21] P. D. Rubin,[32] F. Sabatié,[27,6] C. Salgado,[25] J. P. Santoro,[36,34] V. Sapunenko,[16,34] R. A. Schumacher,[4] V. S. Serov,[18] Y. G. Sharabian,[34] J. Shaw,[22] E. S. Smith,[34] L. C. Smith,[37] D. I. Sober,[5] A. Stavinsky,[18] S. Stepanyan,[34] B. E. Stokes,[11] P. Stoler,[30] S. Strauch,[33] R. Suleiman,[21] M. Taiuti,[16] S. Taylor,[31] D. J. Tedeschi,[33] R. Thompson,[29] A. Tkabladze,[27,26] S. Tkachenko,[27,26] L. Todor,[4] C. Tur,[33] M. Ungaro,[30,8] M. F. Vineyard,[35,32] A. V. Vlassov,[18] D. P. Weygand,[34] M. Williams,[4] E. Wolin,[34] M. H. Wood,[33] A. Yegneswaran,[34] J. Yun,[27] L. Zana,[24] and J. Zhang[27]

(CLAS Collaboration)

JLAB data

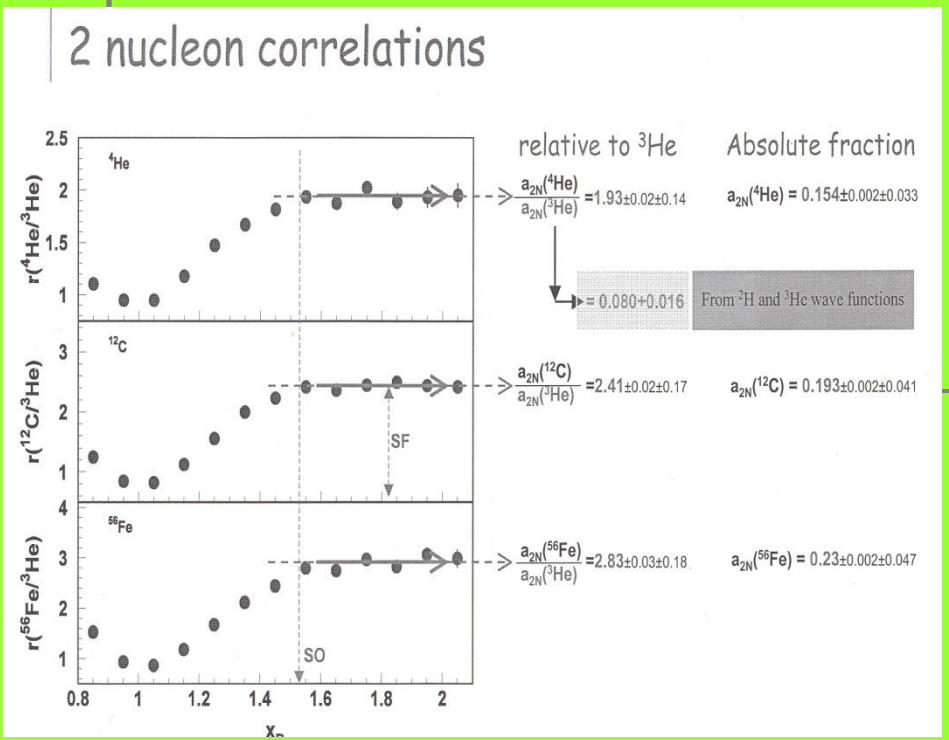
2 nucleon correlations
relative to ³He
Absolute fraction
⁴He
r(⁴He/³He)
a2N(⁴He)/a2N(³He) =1.93±0.02±0.14
a2N(⁴He) = 0.154±0.002±0.033
= 0.080+0.016
From ²H and ³He wave functions
¹²C
r(¹²C/³He)
SF
a2N(¹²C)/a2N(³He) =2.41±0.02±0.17
a2N(¹²C) = 0.193±0.002±0.041
⁵⁶Fe
r(⁵⁶Fe/³He)
SO
a2N(⁵⁶Fe)/a2N(³He) =2.83±0.03±0.18
a2N(⁵⁶Fe) = 0.23±0.002±0.047
0.8 1 1.2 1.4 1.6 1.8 2
xB

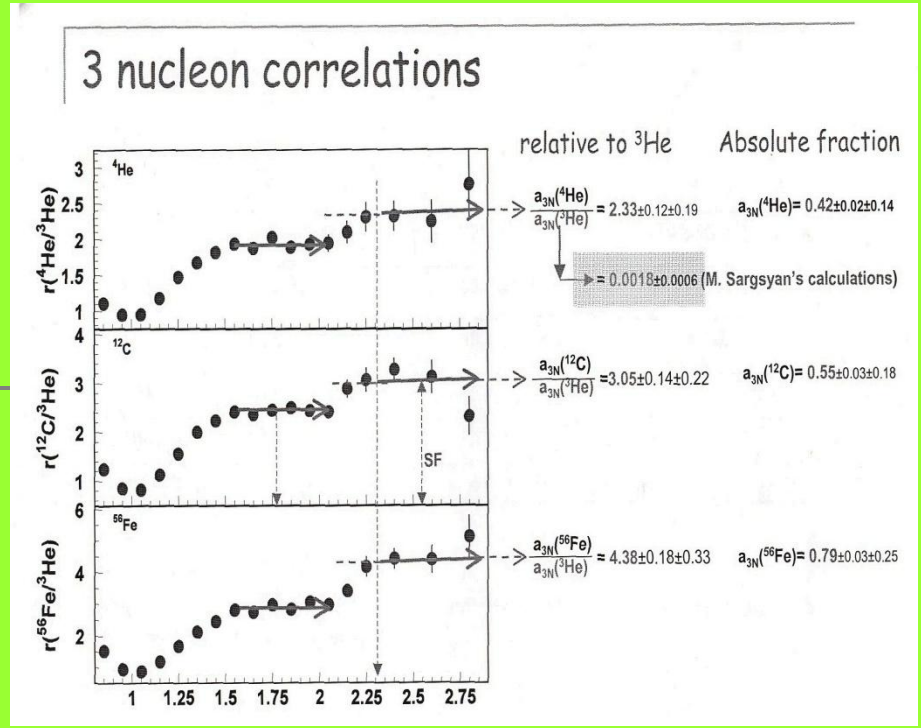
3 nucleon correlations
relative to ³He
Absolute fraction
⁴He
r(⁴He/³He)
a3N(⁴He)/a3N(³He) = 2.33±0.12±0.19
a3N(⁴He)= 0.42±0.02±0.14
= 0.0018±0.0006 (M. Sargsyan's calculations)
¹²C
r(¹²C/³He)
SF
a3N(¹²C)/a3N(³He) =3.05±0.14±0.22
a3N(¹²C)= 0.55±0.03±0.18
⁵⁶Fe
r(⁵⁶Fe/³He)
a3N(⁵⁶Fe)/a3N(³He) = 4.38±0.18±0.33
a3N(⁵⁶Fe)= 0.79±0.03±0.25
1 1.25 1.5 1.75 2 2.25 2.5 2.75

Having these data, we know almost full (≈99%) nucleonic picture of nuclei with $A \leq 56$

Fractions / Nucleus	Single particle (%)	2N SRC (%)	3N SRC (%)
^{56}Fe	**76** ± 0.2 ± 4.7	**23.0** ± 0.2 ± 4.7	**0.79** ± 0.03 ± 0.25
^{12}C	**80** ± 02 ± 4.1	**19.3** ± 0.2 ± 4.1	**0.55** ± 0.03 ± 0.18
^{4}He	**86** ± 0.2 ± 3.3	**15.4** ± 0.2 ± 3.3	**0.42** ± 0.02 ± 0.14
^{3}He	**92** ± 1.6	**8.0** ± 1.6	**0.18** ± 0.06
^{2}H	**96** ± 0.8	**4.0** ± 0.8	-----

Using the published data on (p,2p+n) [PRL,90 (2003) 042301] estimate the isotopic composition of 2N SRC in ^{12}C

$a_{2N}(^{12}C) \approx 20 \pm 0.2 \pm 4.1$ % →

$a_{pp}(^{12}C) \approx 4 \pm 2$ %

$a_{pn}(^{12}C) \approx 12 \pm 4$ %

$a_{nn}(^{12}C) \approx 4 \pm 2$ %

Hadrons probes

V.S. Stavinsky JINR Rapid Communications N18-86, p.5 (1986)

In cumulative processes ☙ $(X_I \cdot M_I) + (X_{II} \cdot M_{II}) \rightarrow m_c + [X_I \cdot M_I + X_{II} \cdot M_{II} + m_2]$

In quark-parton model ☙ $(X_I \cdot P_I) + (X_{II} \cdot P_{II}) \rightarrow m_c + M(X_I, X_{II})$

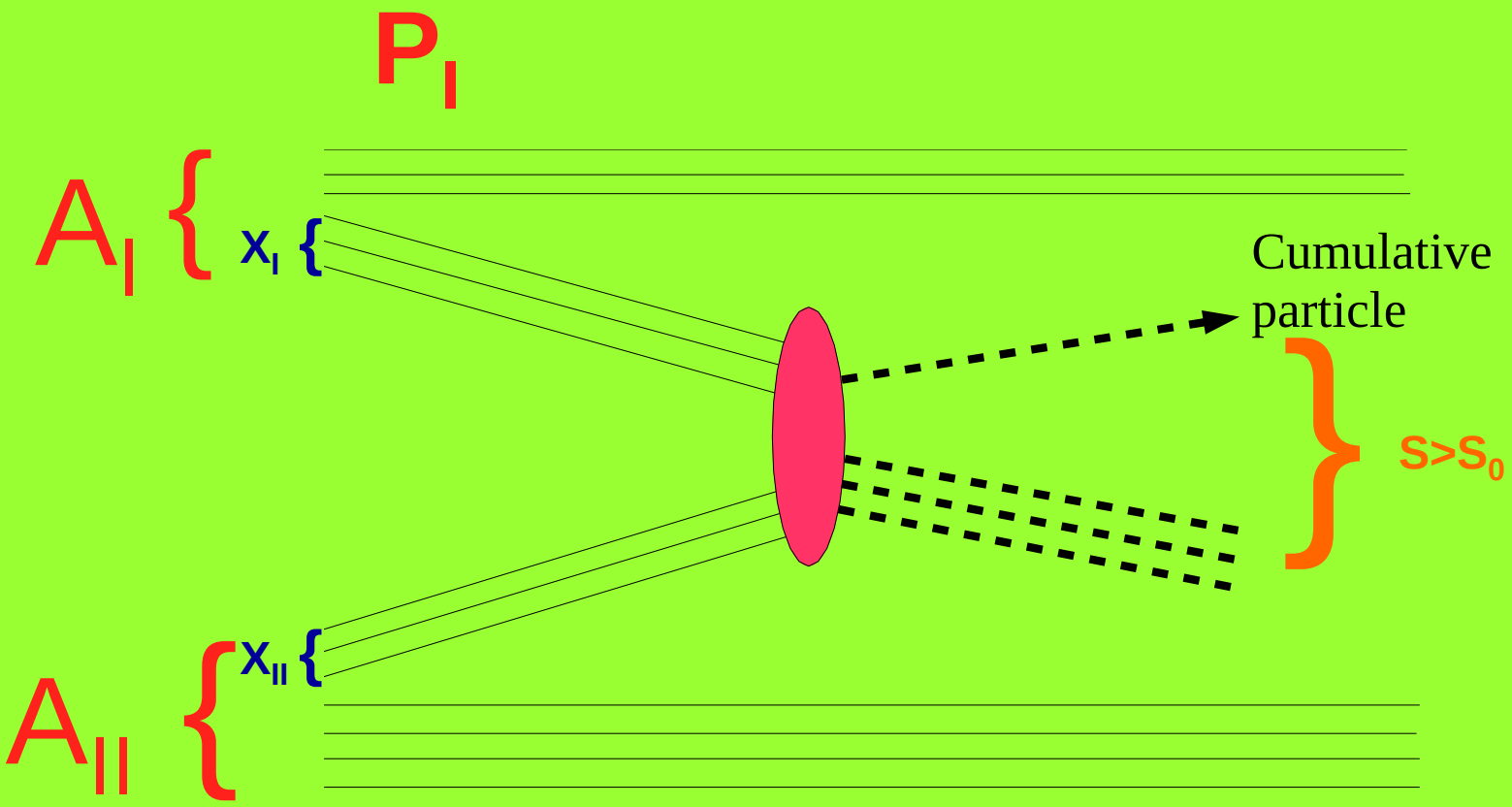

$$s_0 = \left(\frac{\mathbf{P_I}}{\mathbf{A_I}} + \frac{\mathbf{P_{II}}}{\mathbf{A_{II}}}\right)^2$$

Kinematic's limit for free NN-interaction

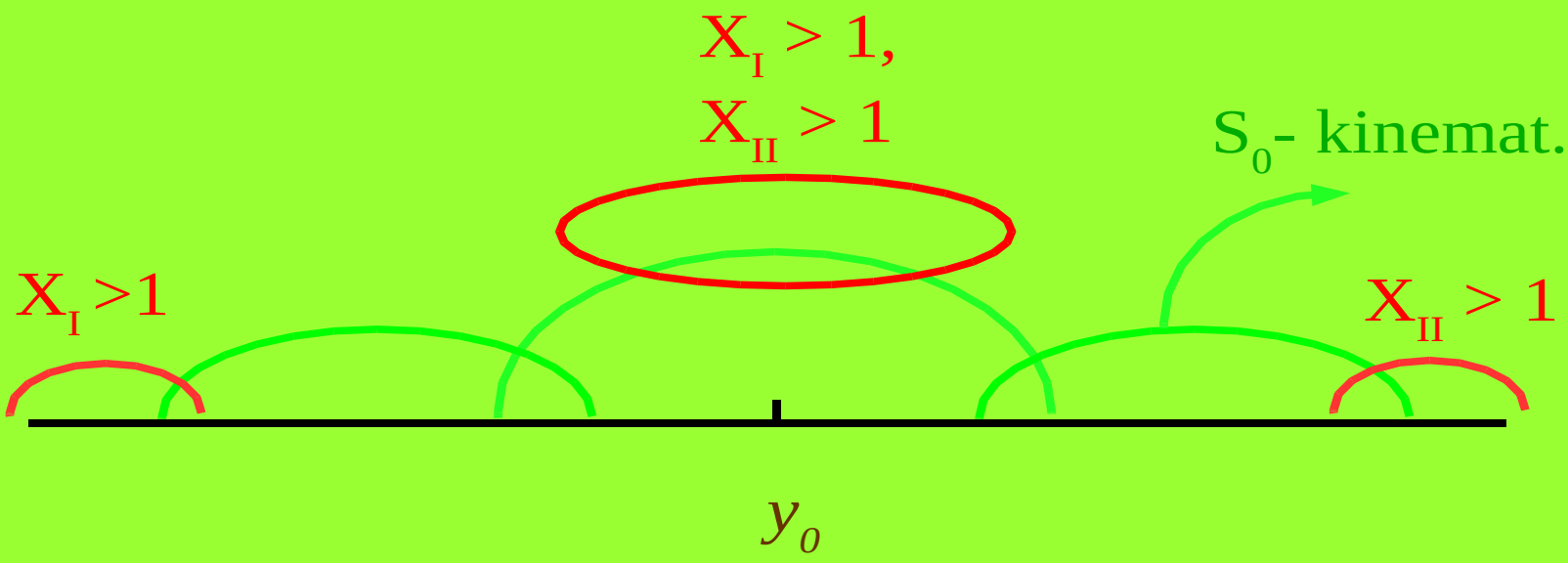

Cumulative processes:

1) $X_I = 1$ and $X_{II} > 1$ } **Fragmentation**
2) $X_{II} = 1$ and $X_I > 1$ } **regions**
3) $X_I > 1$ and $X_{II} > 1$ **Central region**

A.A. Baldin's parameterization

Phys. At. Nucl. 56(3), p.385(1993)

$$\Pi = \frac{1}{2}(X_I^2 + X_{II}^2 + 2 \cdot X_I \cdot X_{II} \cdot \gamma_{I,II})^{\frac{1}{2}} = \frac{1}{2 \cdot m} \cdot S_{\min}^{\frac{1}{2}}$$

$$\gamma_{I,II} = \frac{(P_I \cdot P_{II})}{M_I \cdot M_{II}}$$

Inclusive data parameterization

$$E \cdot \frac{d^3\sigma}{dp^3} = C_1 \cdot A_I^{\frac{1}{3}+\frac{X_I}{3}} \cdot A_{II}^{\frac{1}{3}+\frac{X_{II}}{3}} \cdot \exp(-\frac{\Pi}{C_2}),$$

$$C_1 = 2200[mb \cdot GeV^{-2} \cdot c^3 \cdot sr^{-1}], C_2 = 0.127$$

Cumulative processes.

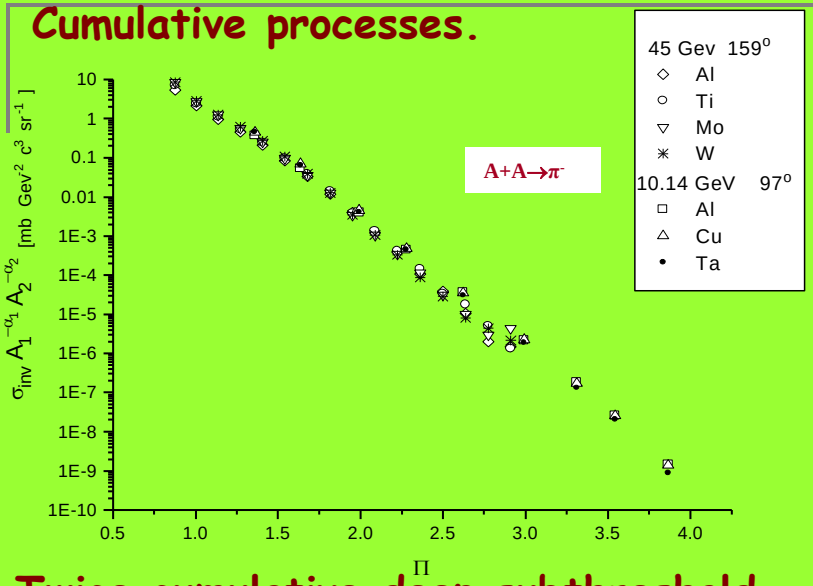

Twice cumulative processes.

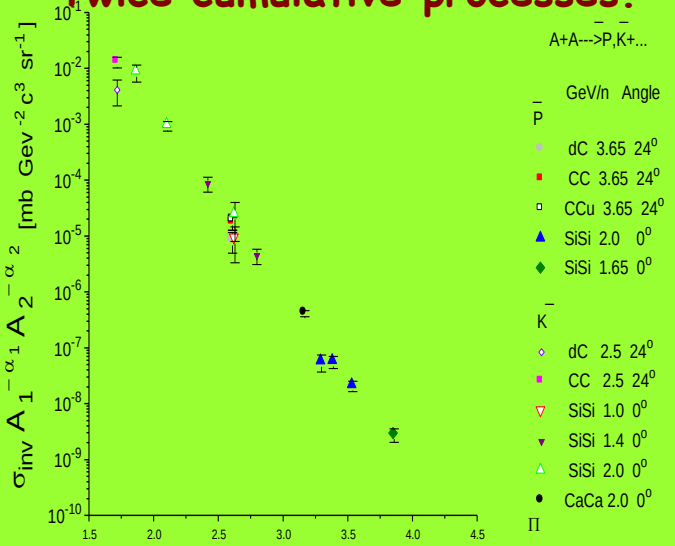

Twice cumulative deep subthreshold processes with heavy nuclei.

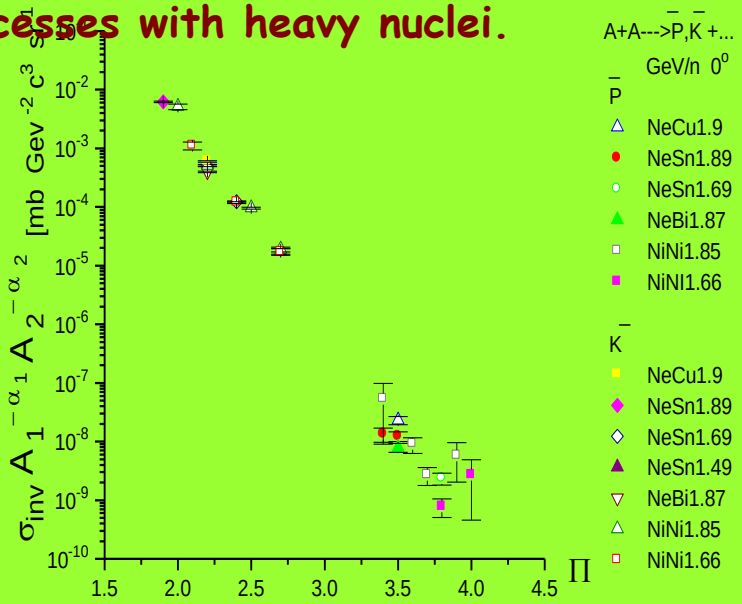

Antimatter production.

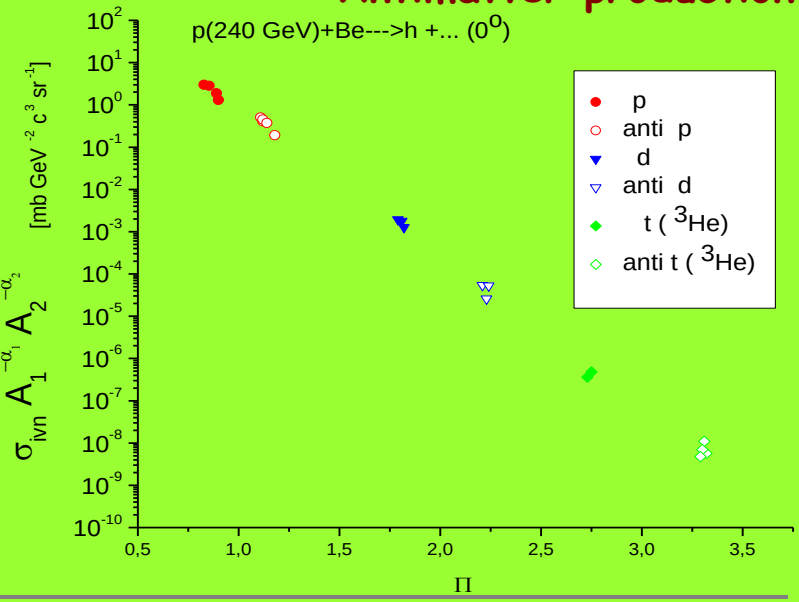

Fluctons

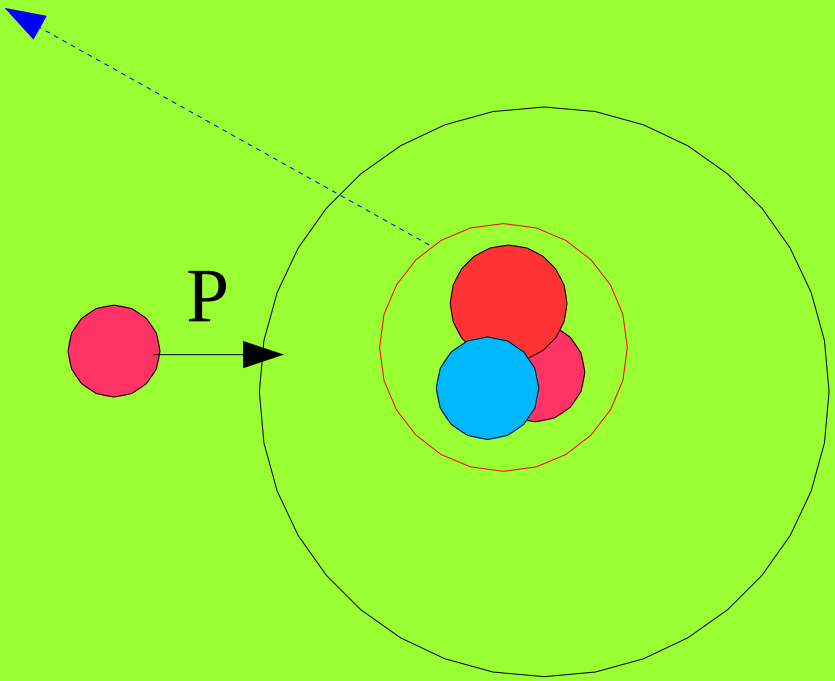

$pA \to h + X$

$$\sigma_h \sim P_K \cdot G_{h/K}(K)$$

Volume 67B, number 1 PHYSICS LETTERS 14 March 1977

ТЕОРИЯ

LARGE MOMENTUM PION PRODUCTION IN PROTON NUCLEUS COLLISIONS AND THE IDEA OF "FLUCTUONS" IN NUCLEI

V.V. BUROV
The Moscow State University, Moscow, USSR
and
V.K. LUKYANOV and A.I. TITOV
Joint Institute for Nuclear Research, Dubna, USSR

Received 27 January 1977

It is shown that in proton-nucleus collisions, the production of pions with large momenta can be explained by the assumption of the existence of nuclear density fluctuations ("fluctuons") at short distances of the nucleon core radius order, with the mass of several nucleons.

The purpose of this note is to realize the idea [4] that the cumulative effect is connected largely with a suggestion on the existence in nuclei of the so-called fluctuons. Earlier fluctuons were proposed [7] in order to understand the nature of the "deuteron peak" in the pA-scattering cross section at large momentum transfers [8] and also to interpret the pd-scattering

cross section [9]. Compressional fluctuations of mass $M_k = km_p$ of nucleons in the small volume $V_\xi = \frac{4}{3}\pi r_\xi^3$ where r_ξ is the fluctuon radius were assumed.

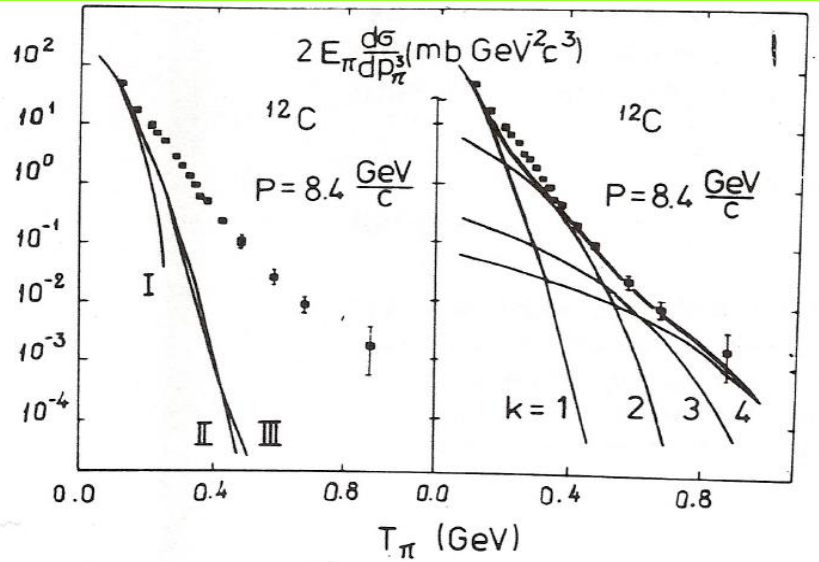

Fig. 1. (a) Calculations of the invariant pion production cross section for ^{12}C: I – for the free proton target; II – with fermi motion; III – the relativization effect. (b) The contributions of separate fluctuons with mass $M_k = km_p$ where k is the order of cumulativity.

Fermi motion and SRC

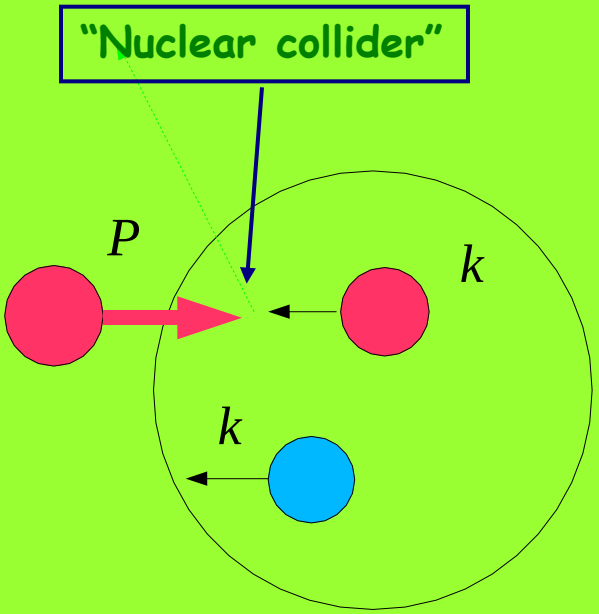

pA -> π, K, $\bar{p}$ ...+ X

$$\sigma_\pi \sim n(\vec{k}) \cdot \sigma(NN \to \pi, K + X)$$

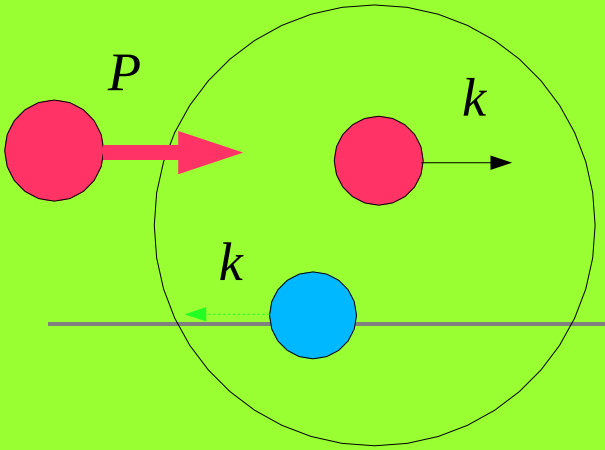

pA -> *p,n* + *X*

$$\sigma_N \sim n(\vec{k}) \cdot \sigma_0$$

Physics of Atomic Nuclei, Vol. 65, No. 11, 2002, pp. 1985–1994. Translated from Yadernaya Fizika, Vol. 65, No. 11, 2002, pp. 2042–2051.

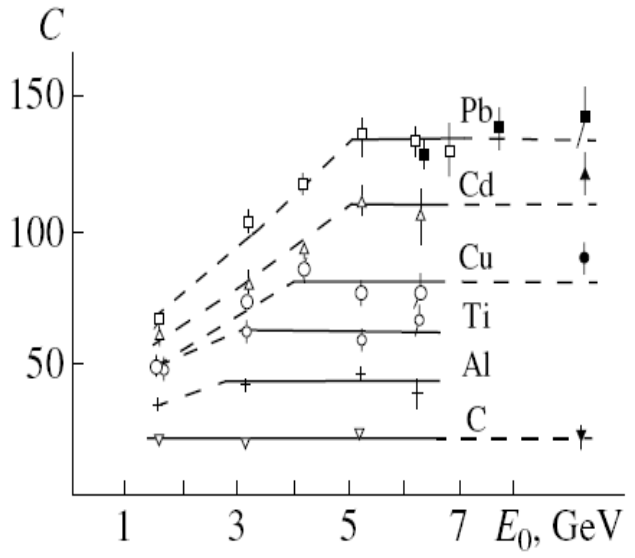

Fig. 3. The coefficient $C(T_0 = 125$ MeV) in the parametrization of the invariant function $f = C\exp(-T/T_0)$ in the reaction pA(C, Al, Ti, Cu, Cd, Pb) $\rightarrow pX$ for a proton escape angle of 120° in the laboratory frame versus the incident-proton energy. The filled circles refer to the initial energy of 400 GeV.

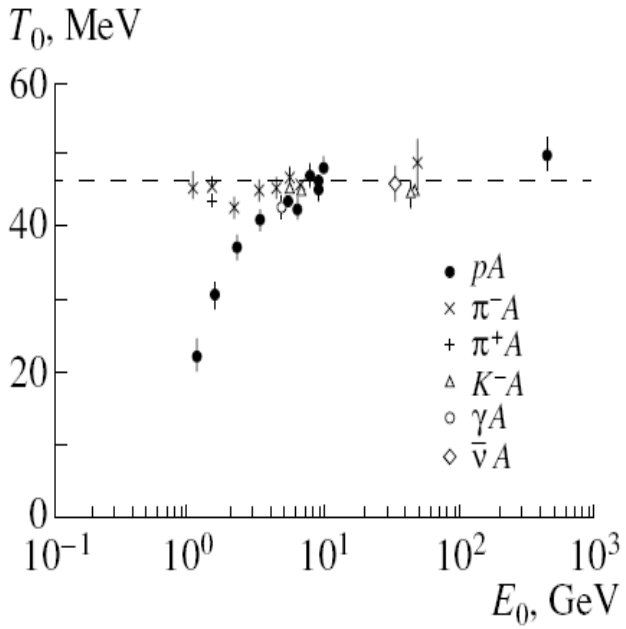

Fig. 5. Dependence of the slope parameter T_0 for the invariant function of the protons escaping under the action of $p, \pi^{\pm}, K^-, \gamma, \bar{\nu}$ with various energies E_0; the escape angle is 120° in the laboratory frame.

VOLUME 43, NUMBER 24 PHYSICAL REVIEW LETTERS 10 DECEMBER 1979

Energy Dependence of Charged Pions Produced at 180° in 0.8–4.89-GeV Proton-Nucleus Collisions

L. S. Schroeder, S. A. Chessin, J. V. Geaga, J. Y. Grossiord,[a]
J. W. Harris, D. L. Hendrie, R. Treuhaft, and K. Van Bibber
Lawrence Berkeley Laboratory, University of California, Berkeley, California 94720
(Received 25 September 1979)

High-energy charged pions produced at 180° in 0.8–4.89-GeV proton-nucleus collisions have been studied. Both the slopes of the energy spectra and the π^-/π^+ ratios increase rapidly with primary energy up to ~3–4 GeV, where limiting values appear to be reached. The dependence on target mass also changes over this energy range. Unlike forward pion-production results, backward pions at these energies do not obey the scaling law suggested by Schmidt and Blankenbecler.

We report on a systematic study of the energy dependence of charged pions produced at 180° in the collisions of 0.8–4.89-GeV protons with nuclei. A principal reason for studying production of energetic pions from nuclei in the backward direction is that in free nucleon-nucleon (N-N) collisions such production is kinematically restricted. Observation of pions beyond this kinematic limit may then be evidence for exotic production mechanisms such as production from clusters.[1-5] Early experiments by Baldin *et al.*[6] using 5.14- and 7.52-GeV protons observed

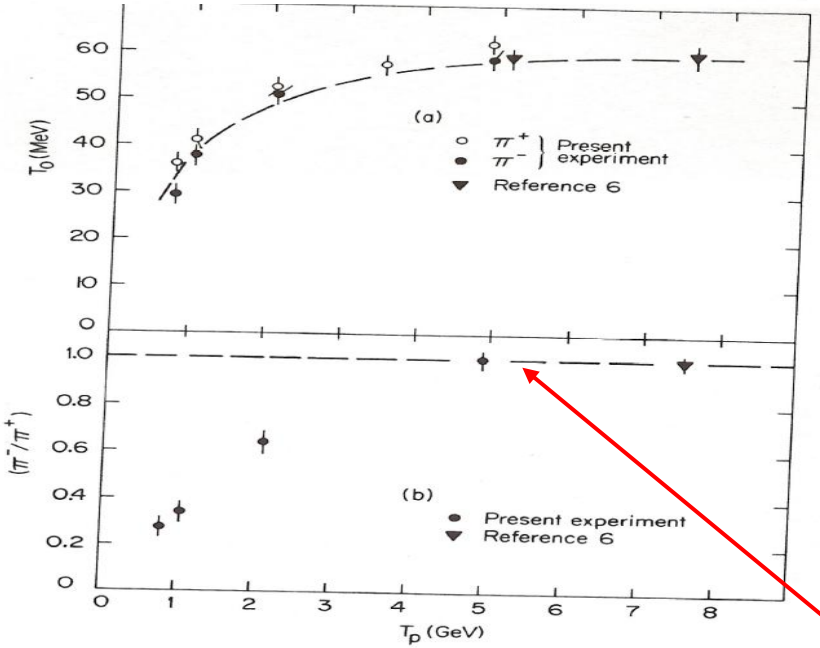

FIG. 1. Energy dependence of (a) T_0 parameter for pions, and (b) the π^-/π^+ ratio at 180° obtained by integrating each spectra up to 100 MeV for p-Cu collisions from 0.8 to 4.89 GeV. The dashed curve in both cases refers to the predictions of the "effective-target" model (Refs. 3 and 4).

tering mechanism to one where nucleon clusters play an ever increasing role. To isolate the production mechanism further, experiments are required which will measure additional observables such as associated multiplicities and two-particle correlations. However, it is clear that by measuring the production of pions in kinematic regions beyond those available in free N-N collisions, such as at 180° and high energies, one is probing the short-range behavior of nucleons in nuclei. This behavior might manifest itself as large Fermi momenta or nucleon clusters.

Isotopic scalar state

Isotopic scalar state

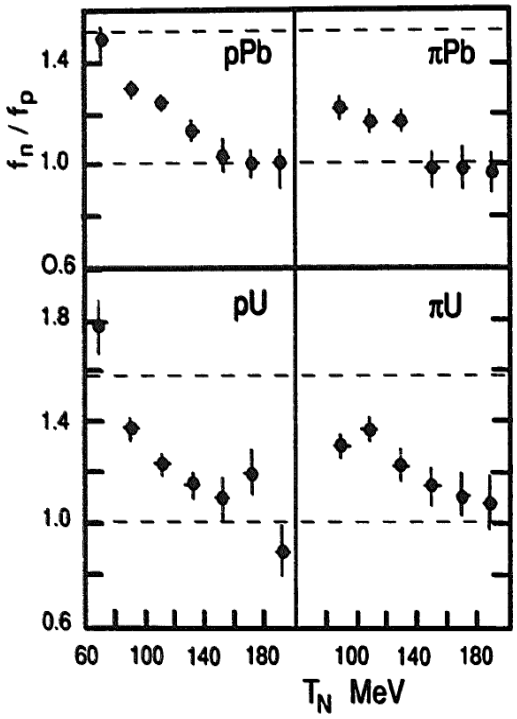

Figure 3 : Ratio of neutron to proton yields for various nuclei and various probes, as a function of the energy of the secondary hadron

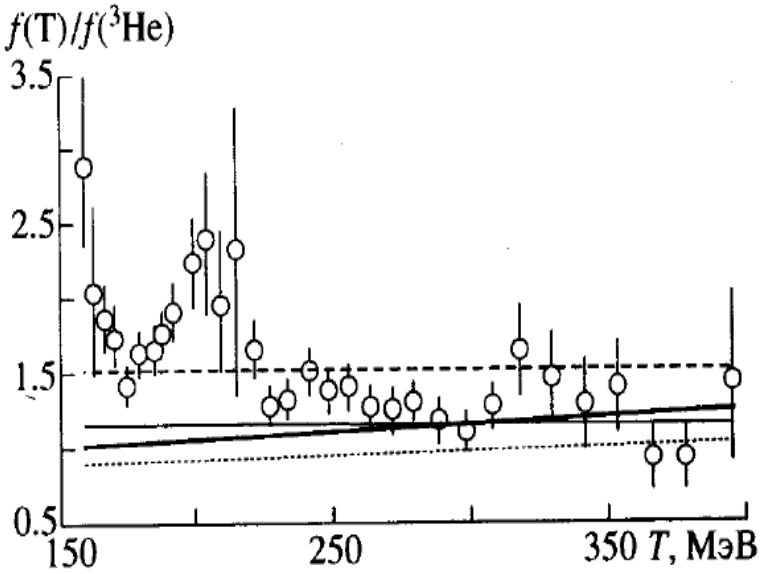

Рис. 9. Зависимость отношения $T/^3He$ от кинетической энергии вторичных частиц. Угол $\theta = 90°$, ядро – Pb. Обозначения кривых аналогичны рис. 1.

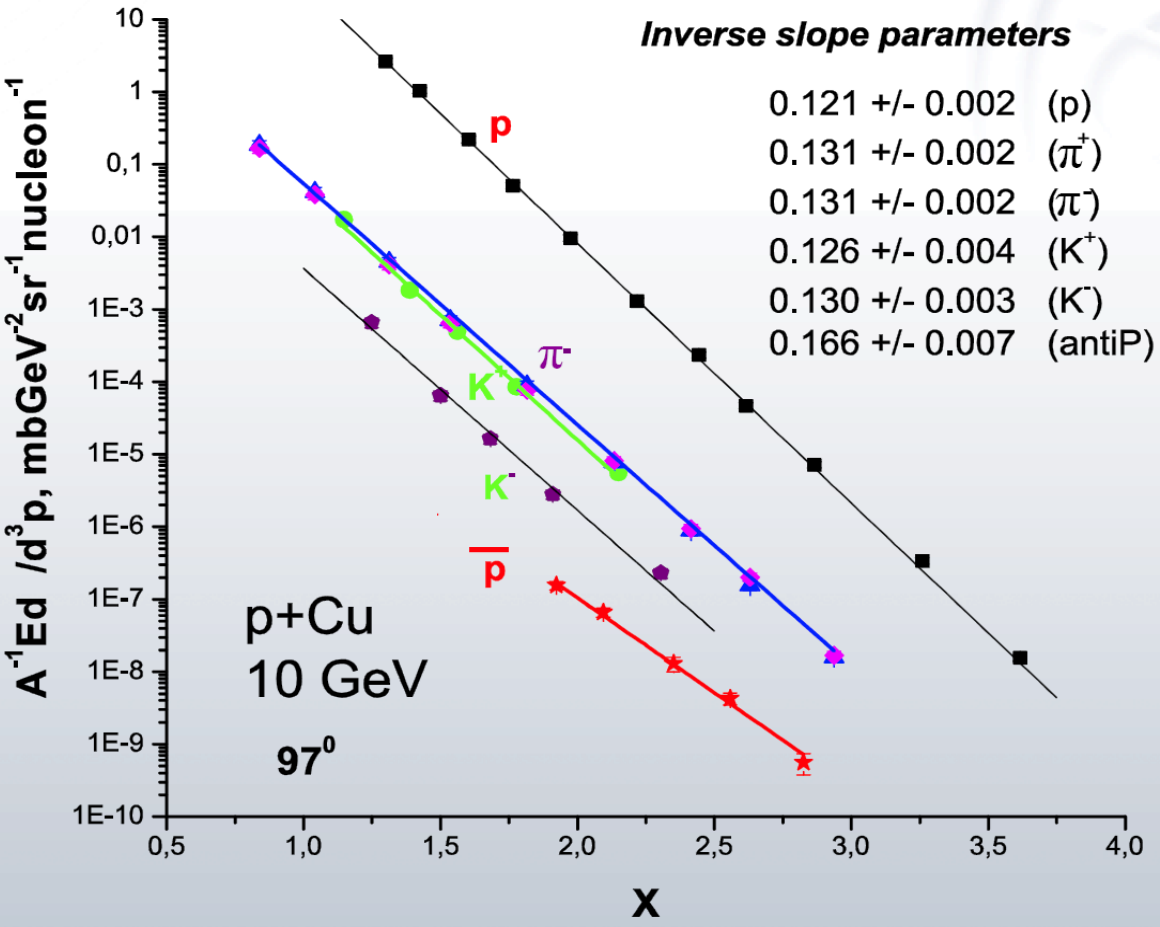

FAS @ ITEP (Boyarinov et.al Yad.Fiz 57 (1994) 1452)

X – minimal target mass [m_N] needed to produce particle

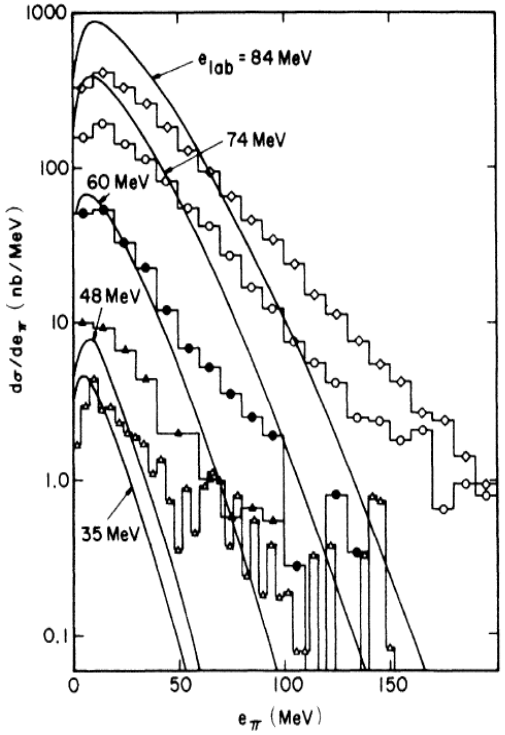

FIG. 2. Comparison of calculated and experimenta spectra. The input π^0 absorption cross sections are those by the upper solid curve in Fig. 1. For the lower solid cu that figure, the results shown here must be scaled dow factor of about 2. The data are taken from Refs. 6 and the reaction $^{12}C+^{12}C$ (upper four curves) and from Ref. the reaction $^{14}N + Ni$ (open triangles).

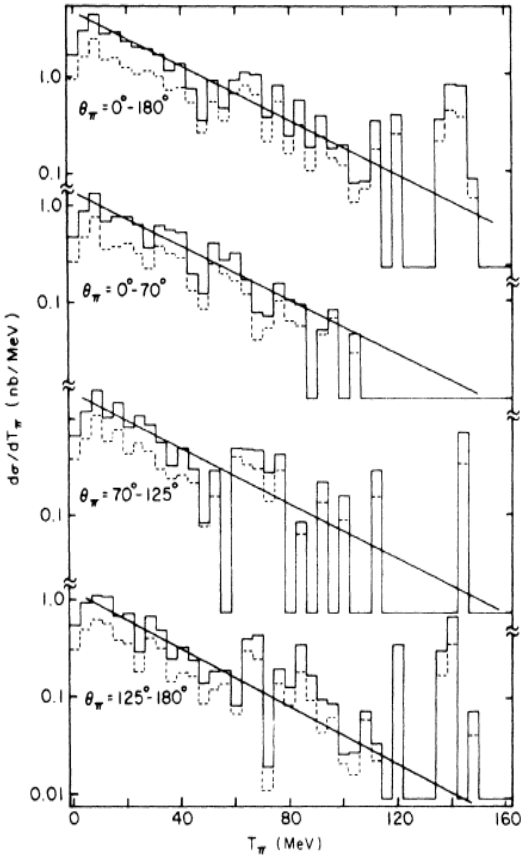

FIG. 3. Pion kinetic energy spectrum (solid histogram) in the laboratory frame for 35 MeV/nucleon $^{14}N+Ni$ integrated over all pion emission angles θ_π (top) and for various θ_π bins. For the meaning of the dashed histograms see the text. The straight lines represent an exponential with an inverse slope constant of 23 MeV.

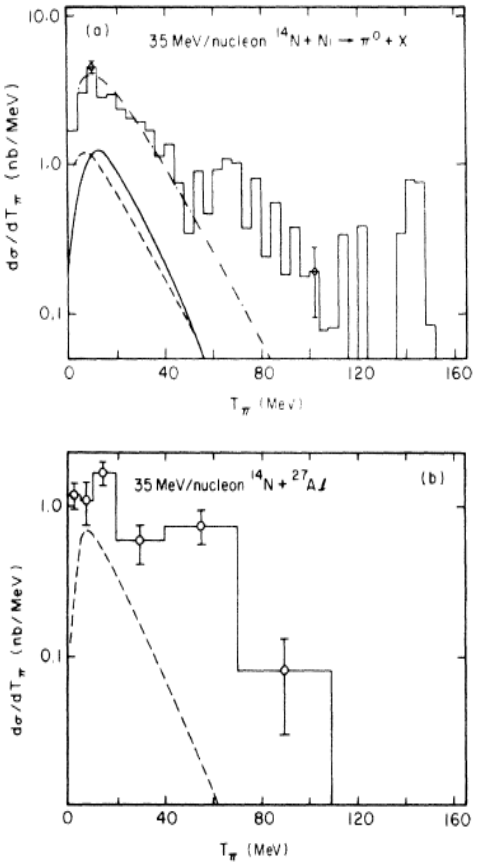

FIG. 4. Experimental pion kinetic energy spectra at 35 MeV/nucleon for the Ni and Al target. The spectrum for the Al target corresponds to the same measurements as shown in Ref. 6 but differs from the spectrum shown there by subtraction of the cosmic-ray background and use of the energy dependent conversion efficiency as discussed in the text (as compared to no cosmic subtraction and $\epsilon_c = 0.7$). The solid and dashed lines are predictions of Refs. 27 and 30, respectively. The dashed dotted line corresponds to a thermal spectrum (Ref. 20) with $T = 12.2$ MeV and is normalized to the data at low kinetic energies (10–60 MeV).

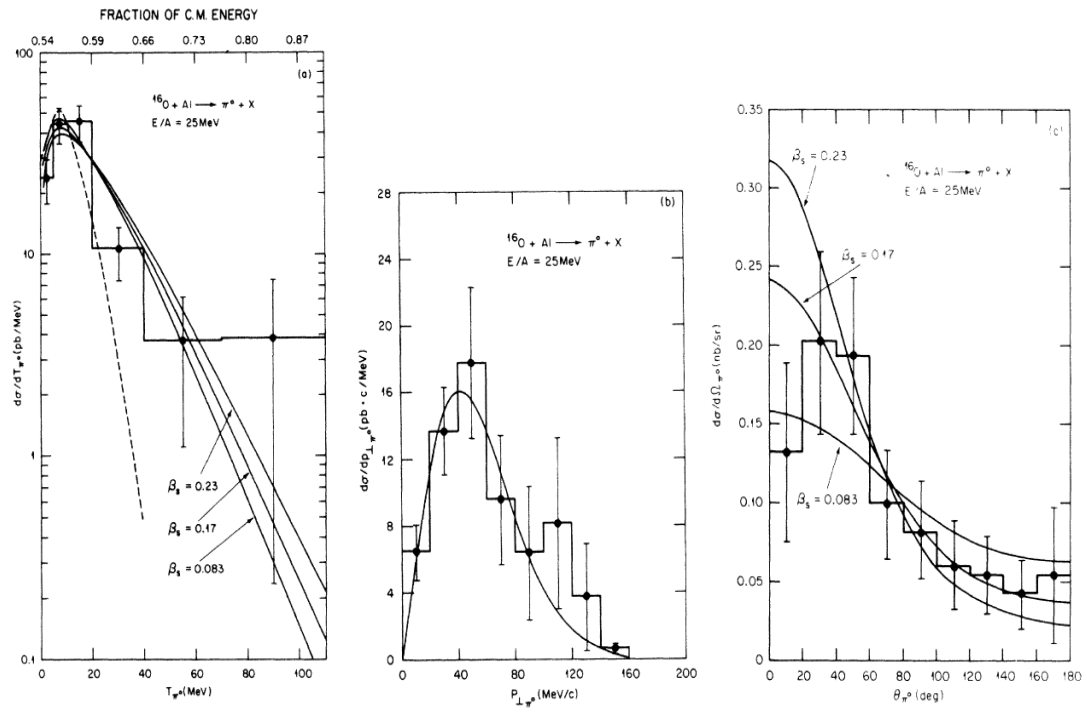

FIG. 2. (a) Laboratory kinetic energy distribution, (b) transverse momentum distribution, and (c) angular distribution for neutral pions observed in the reaction $E_{lab}/A = 25$ MeV $^{16}O + Al \rightarrow \pi^0 + K$. The dashed line in (a) is the prediction of Ref. 9 multiplied by a factor of 50. The solid line in (b) is a fit using Eq. (1) and yields $T = 11.6$ MeV. The solid lines in (a) and (c) are predictions of the simple thermal model discussed in the text with $T = 11.6$ MeV and source speeds $\beta_s = 0.083$, 0.17, and 0.23. The legend at the top of (a) is the fraction of the c.m. energy required to produce a π^0 traveling at 0° in the laboratory.

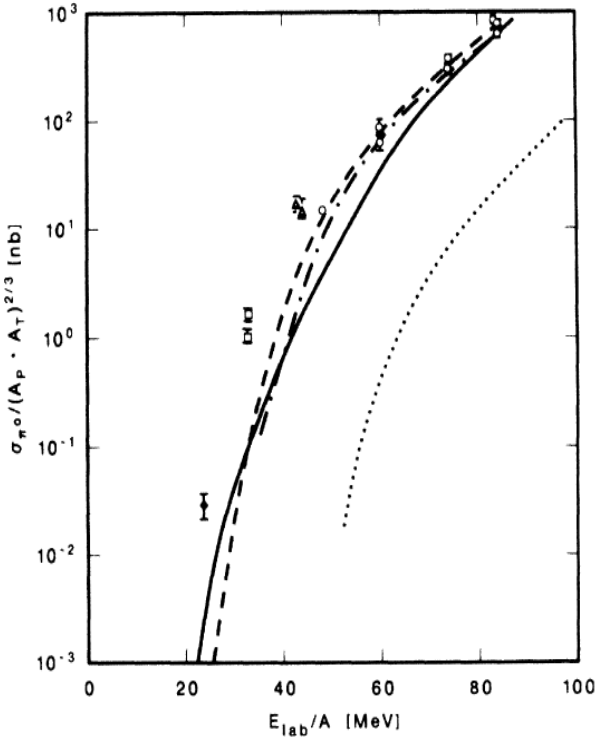

FIG. 3. Inclusive cross section for π^0 production, divided by $(A_p^{2/3} A_T^{2/3})$, where A_p and A_T are the projectile and target mass numbers, respectively, as a function of laboratory bombarding energy. (Open circles, Ref. 3; open triangles, Ref. 4; open squares, Ref. 2; closed diamond, present work.) The theoretical curves are from Ref. 8 (dotted line), Ref. 9 (long dashed line), Ref. 11 (dash-dot line), and Ref. 12 (solid line).

PHYSICAL REVIEW C VOLUME 33, NUMBER 4 APRIL 1986

Pion production: A probe for coherence in medium-energy heavy-ion collisions

J. Stachel, P. Braun-Munzinger, R. H. Freifelder,* P. Paul, S. Sen, P. DeYoung,† and P. H. Zhang‡
Department of Physics, State University of New York at Stony Brook, Stony Brook, New York 11794

T. C. Awes, F. E. Obenshain, F. Plasil, and G. R. Young
Physics Division, Oak Ridge National Laboratory, Oak Ridge, Tennessee 37831

R. Fox and R. Ronningen
National Superconducting Cyclotron Laboratory, Michigan State University, East Lansing, Michigan 48824

(Received 19 November 1985)

The production of neutral pions has been studied in reactions of 35 MeV/nucleon $^{14}N+^{27}Al,Ni,W$ and 25 MeV/nucleon $^{16}O+^{27}Al,Ni$. Inclusive pion differential distributions $d\sigma/dT_\pi$, $d\sigma/d\Omega$, $d\sigma/dy$, $d\sigma/dp_\perp$, and $d^2\sigma/dy\,dp_\perp$ have been measured by detecting the two pion-decay γ rays in a setup of 20 lead glass Čerenkov detector telescopes. Special care was taken to understand and suppress background events. Effects of pion reabsorption are discussed and it is found that the cross sections presented here are substantially affected by such final state interactions. The comparatively large experimental cross sections and the shape of the spectral distributions cannot be accounted for in single nucleon-nucleon collision or statistical models; they rather call for a coherent pion production mechanism.

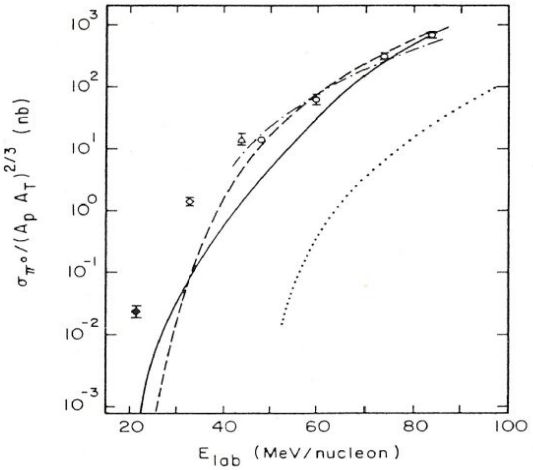

FIG. 13. Experimental integrated pion production cross sections divided by $(A_P A_T)^{2/3}$ for different beam energies. The different symbols signify $^{16}O + ^{27}Al,Ni$ (closed diamond, present data), $^{14}N+^{27}Al,Ni,W$ (open diamond, present data), $^{40}Ar + ^{40}Ca$ (open triangle, Ref. 9), and $^{12}C + ^{12}C$ (open circles, Refs. 8 and 10). Also shown are results of a single nucleon-nucleon hard scattering model (Ref. 23) (dotted line), the extended phase space model (Ref. 27) (dashed line), a thermal model (Ref. 30) (solid line), and the bremsstrahlung model (Ref. 38) (dashed dotted line).

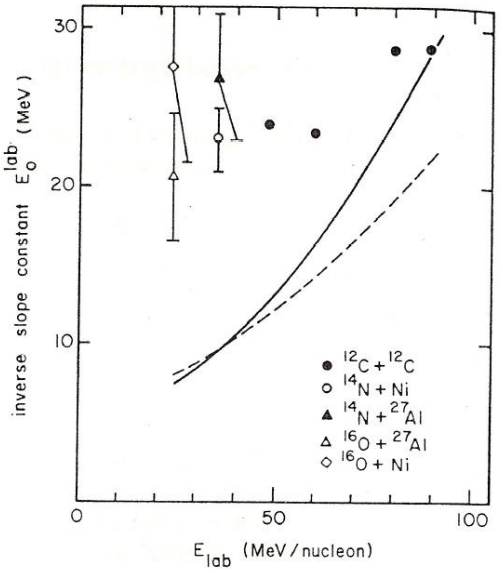

FIG. 14. Experimentally determined slope constants E_0 of pion kinetic energy spectra plotted as a function of beam energy/nucleon. For C + C spectra see Refs. 8 and 10. The solid and dashed lines correspond to predictions of Refs. 30 and 27, respectively. For details see the text.

Subthreshold flucton-flucton production

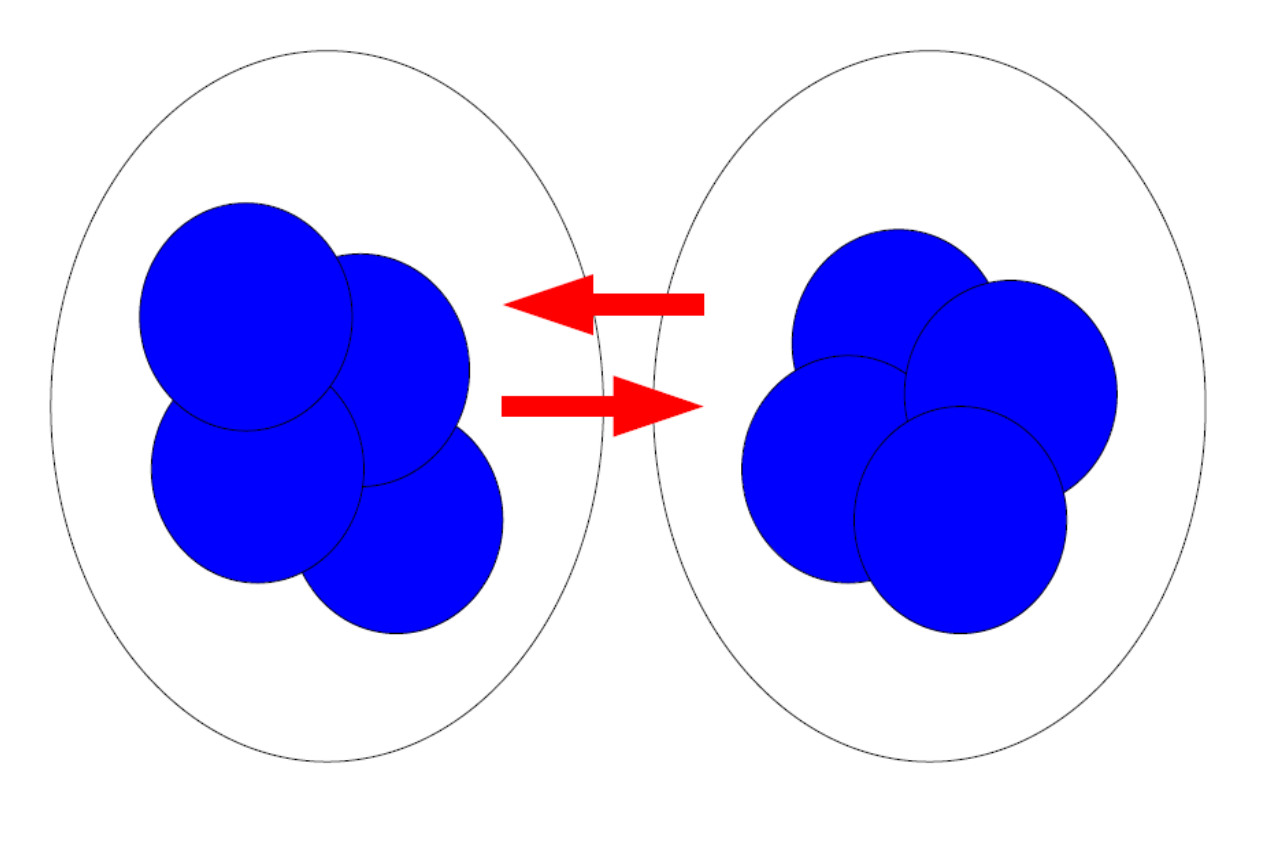

$$\sigma_h \sim P^2{}_K \cdot G^2{}_{h/K}(K)$$

Inverse slope for subthreshold production must be the less then $T_0/2$ (near the phase space border).

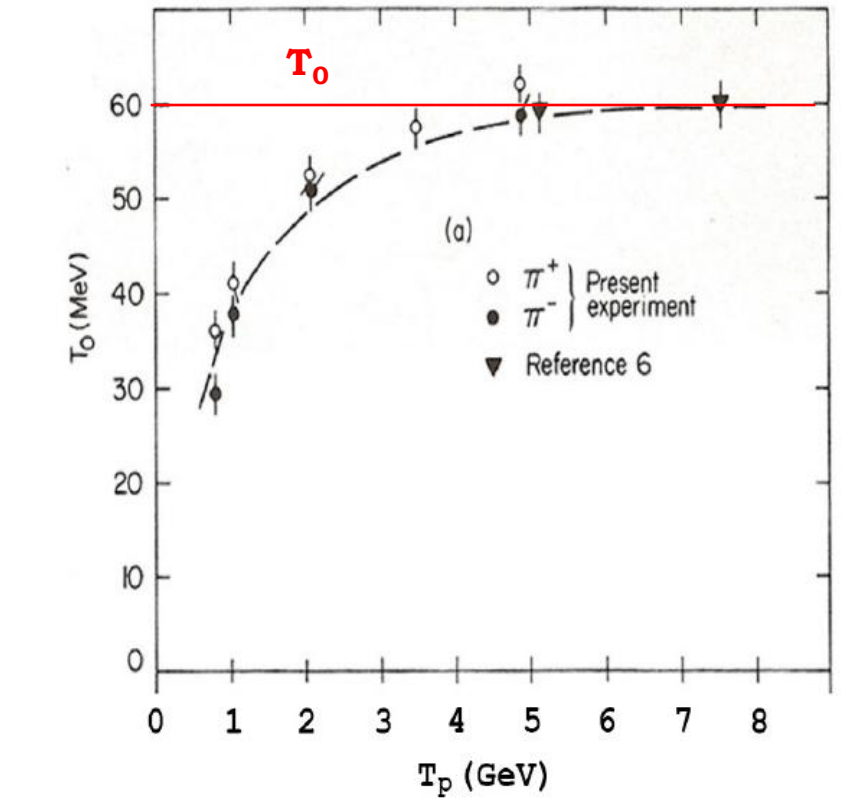

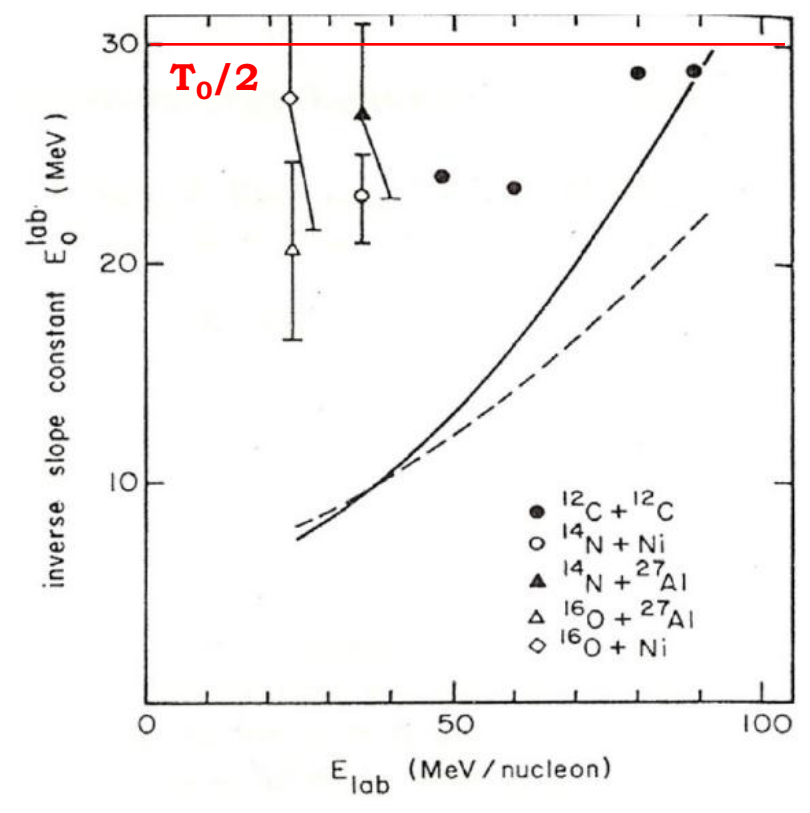

$$P_{cum} \sim \exp\left(-T/T_0\right) \quad \Rightarrow \quad P_{subthresh} \sim \exp\left(-T/T_0\right) \cdot \exp\left(-T/T_0\right) \sim \exp\left(-T/(T_0/2)\right)$$

DINR at high p_T as probes of the cold dense nuclear matter ($x_T \geq 1$)

E850/EVA (BNL)

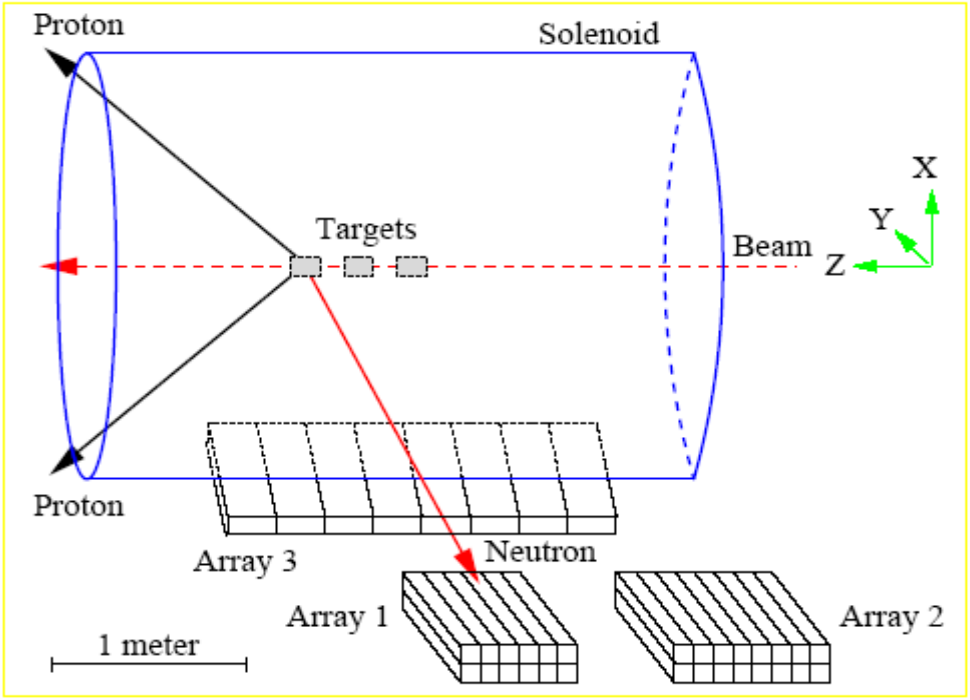

Figure I.3: A schematic view of the EVA solenoid and the neutron counters in the 1998 measurement.

VOLUME 90, NUMBER 4 PHYSICAL REVIEW LETTERS week ending 31 JANUARY 2003

n-p Short-Range Correlations from $(p, 2p + n)$ Measurements

A. Tang,[1] J.W. Watson,[1] J. Aclander,[2] J. Alster,[2] G. Asryan,[4,3] Y. Averichev,[8] D. Barton,[4] V. Baturin,[6,5] N. Bukhtoyarova,[4,5] A. Carroll,[4] S. Gushue,[4] S. Heppelmann,[6] A. Leksanov,[6] Y. Makdisi,[4] A. Malki,[2] E. Minina,[6] I. Navon,[2] H. Nicholson,[7] A. Ogawa,[6] Yu. Panebratsev,[8] E. Piasetzky,[2] A. Schetkovsky,[6,5] S. Shimanskiy,[8] and D. Zhalov[6]

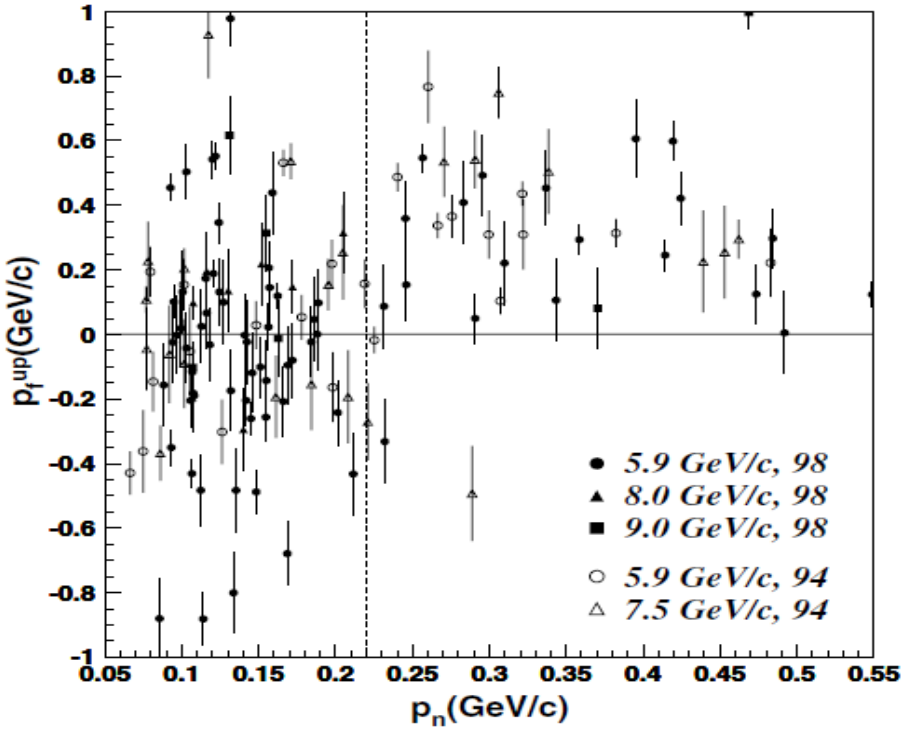

FIG. 1. Scatter plot of p_f^{up} vs p_n with cuts (i), (ii), (iii), (iv), and (v) (see text) for $^{12}C(p, 2p + n)$ events. Data labeled "98" (solid symbols) are for this work. Data labeled "94" are from Aclander *et al.* [2]. The vertical dashed line at 0.22 GeV/c corresponds to k_F, the Fermi momentum for ^{12}C.

Knot out cold dense nuclear configurations

SRC configuration

Multiquark configuration

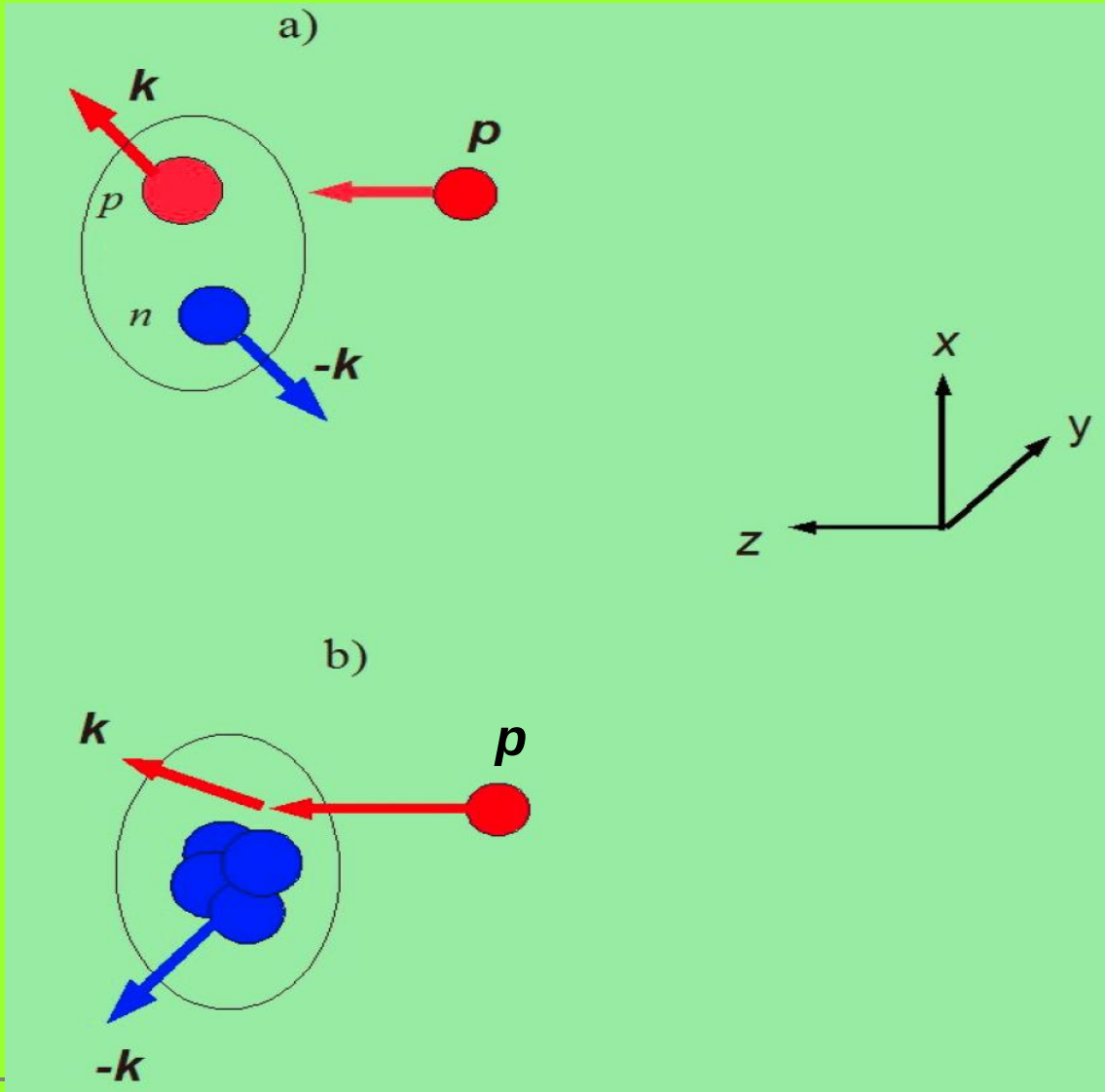

$CT\ (x_T = 1)$

Color(nuclear) transparency in 90^0 c.m. quasielastic $A(p,2p)$ reactions

*The incident momenta varied from 5.9 **to** 14.4 GeV/c, **corresponding to** $4.8 < Q^2 < 12.7$ $(GeV/c)^2$.*

$$T = \frac{\frac{d\sigma}{dt}(p + \text{"}p\text{"} \rightarrow p + p)}{Z\frac{d\sigma}{dt}(p + p \rightarrow p + p)}$$

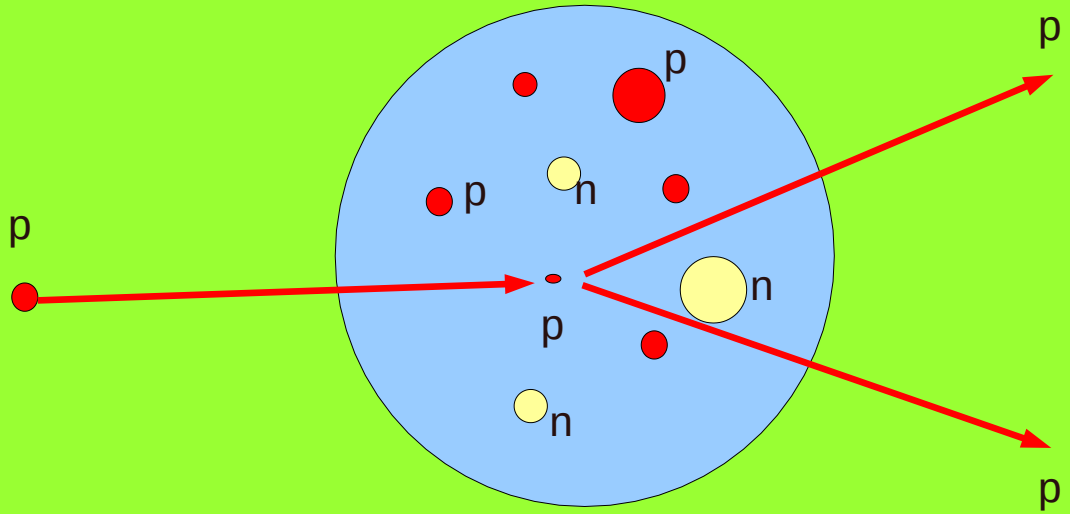

VOLUME 87, NUMBER 21 PHYSICAL REVIEW LETTERS 19 NOVEMBER 2001

Energy Dependence of Nuclear Transparency in C(p,2p) Scattering

A. Leksanov,[5] J. Alster,[1] G. Asryan,[3,2] Y. Averichev,[8] D. Barton,[3] V. Baturin,[5,4] N. Bukhtoyarova,[3,4] A. Carroll,[3] S. Heppelmann,[5] T. Kawabata,[6] Y. Makdisi,[3] A. Malki,[1] E. Minina,[5] I. Navon,[1] H. Nicholson,[7] A. Ogawa,[5] Yu. Panebratsev,[8] E. Piasetzky,[1] A. Schetkovsky,[5,4] S. Shimanskiy,[8] A. Tang,[9] J. W. Watson,[9] H. Yoshida,[6] and D. Zhalov[5]

B.Van Overmeire, J.Ryckebusch, nucl-th/0608040

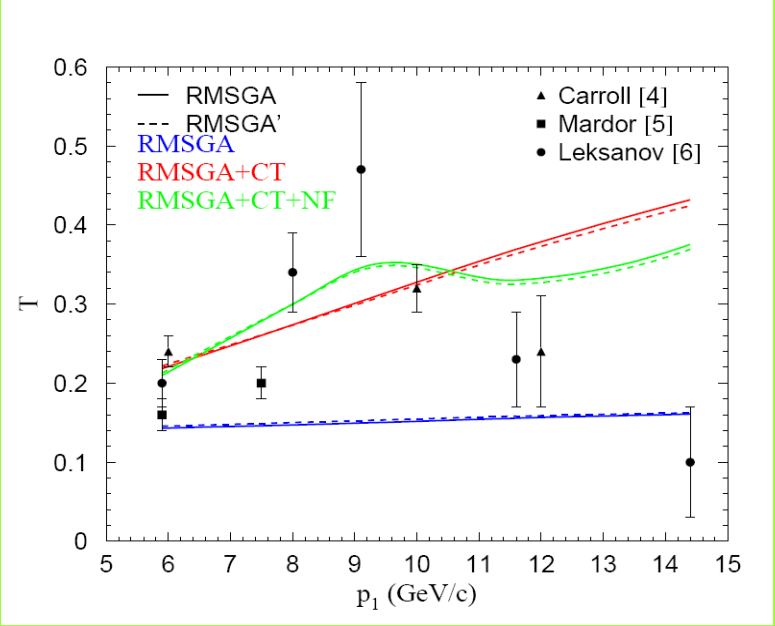

J. Aclander et al., Phys.Rev. C 70, 015208 (2004)

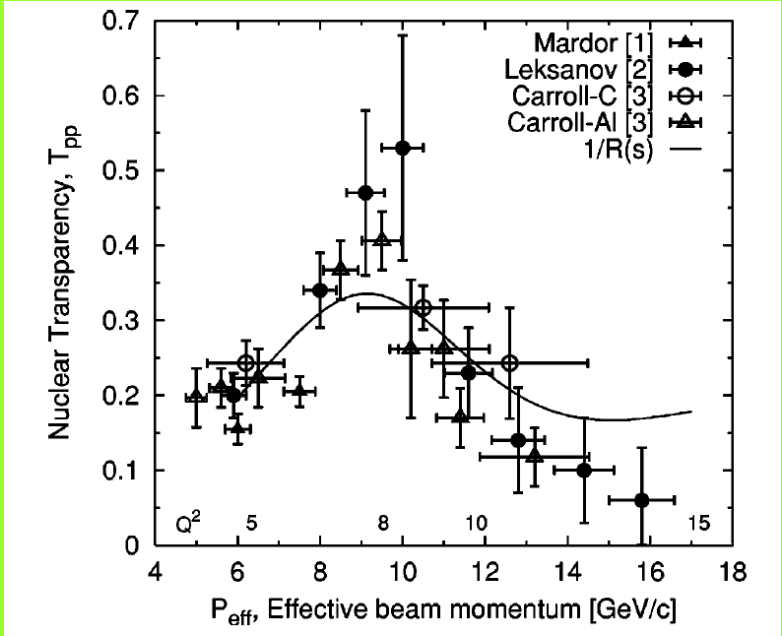

COLOR TRANSPARENCY

PHYSICAL REVIEW C **70**, 015208 (2004)

VIII. SUGGESTIONS FOR FUTURE EXPERIMENTS

Clearly there remain a number of interesting investigations involving nuclear transparency of protons and other hadrons. A revival of the AGS fixed target program [44], or the construction of the 50-GeV accelerator as part of the J-PARC complex in Japan [55], would provide excellent opportunities to expand the range of these nuclear transparency studies. Some of the remaining questions are the following.

(1) What happens at higher incident momentum? Does nuclear transparency rise again above 20 GeV/c, as predicted in the Ralston-Pire picture [56]?

(2) A-dependent studies in the 12 to 15 GeV/c range; will the effective absorption cross section continue to fall after the nuclear transparency stops rising at ~9.5 GeV/c [56]?

(3) At the higher energy ranges of these experiments the spin effects are expected to be greatly diminished. However, they continue to persist, as shown in both single and double spin measurements [34,57]. So it is important to see, in quasielastic scattering inside a nucleus, whether a relatively pure pQCD state is selected, and if the spin dependent effects are attenuated.

(4) Measurements of nuclear transparency with antiprotons, pions, and kaons will be informative. These particles have widely different cross sections at $90^{\circ}_{\text{c.m.}}$. For instance, the pp differential cross section at $90^{\circ}_{\text{c.m.}}$ is 50 times larger than the $\overline{p}\overline{p}$ differential cross section [19]. How should this small size of the $\overline{p}\overline{p}$ cross section affect the absorption of $\overline{p}$'s by annihilation?

(5) The production of exclusively produced resonances provides a large testing ground for nuclear transparency effects. This is especially true for those resonances that allow the determination of final state spin orientation, such as ρ's or Λ's [19,36]. Will the interference terms that generate asymmetries disappear for reactions which take place in the nucleus?

(6) Measurements in light nuclei that determine the probability of a second hard scatter after the first hard interaction are an alternative way to study nuclear transparency effects. With the proper kinematics selected, the probability of the second scatter is dependent on the state of the hadrons at the first hard interaction [58].

Which high p_T problems for spin are interesting in our energy range?

"Spin crisis" of 70's

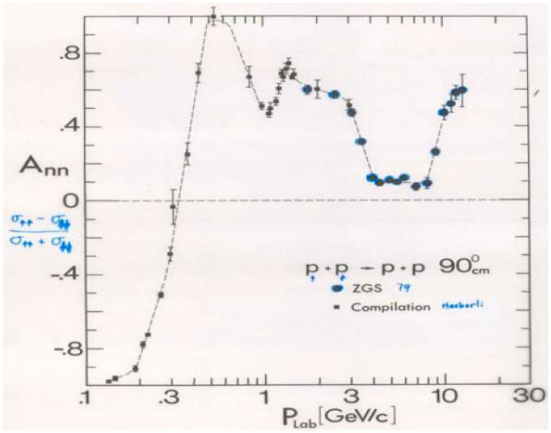

Figure 4: A_{nn} is plotted against P_{Lab}.

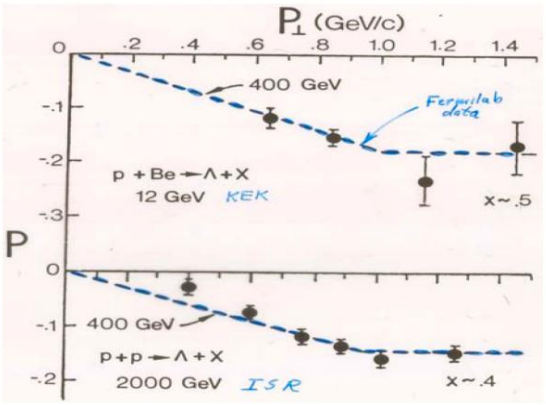

Figure 6: The Λ polarization is plotted against P_t^2.

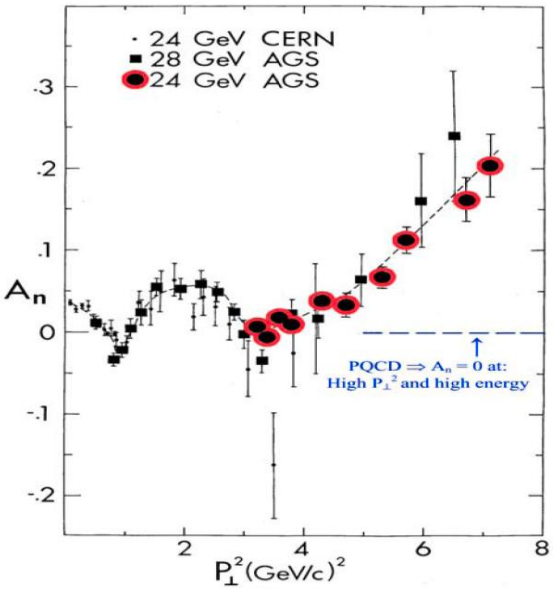

Figure 5: A_n is plotted against P_t^2.

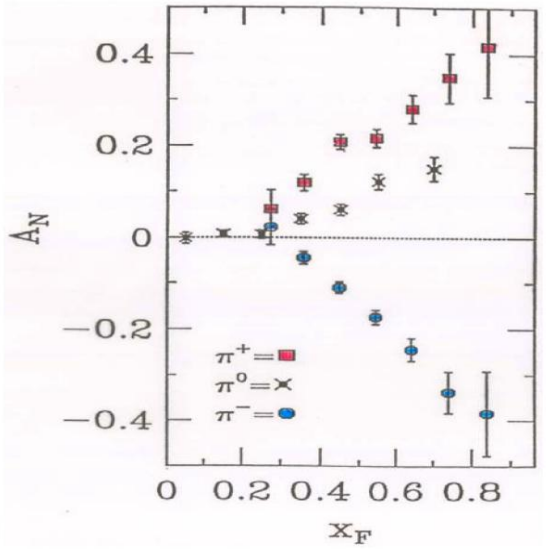

Figure 7: A_n is plotted against X_F for inclusive π-meson production.

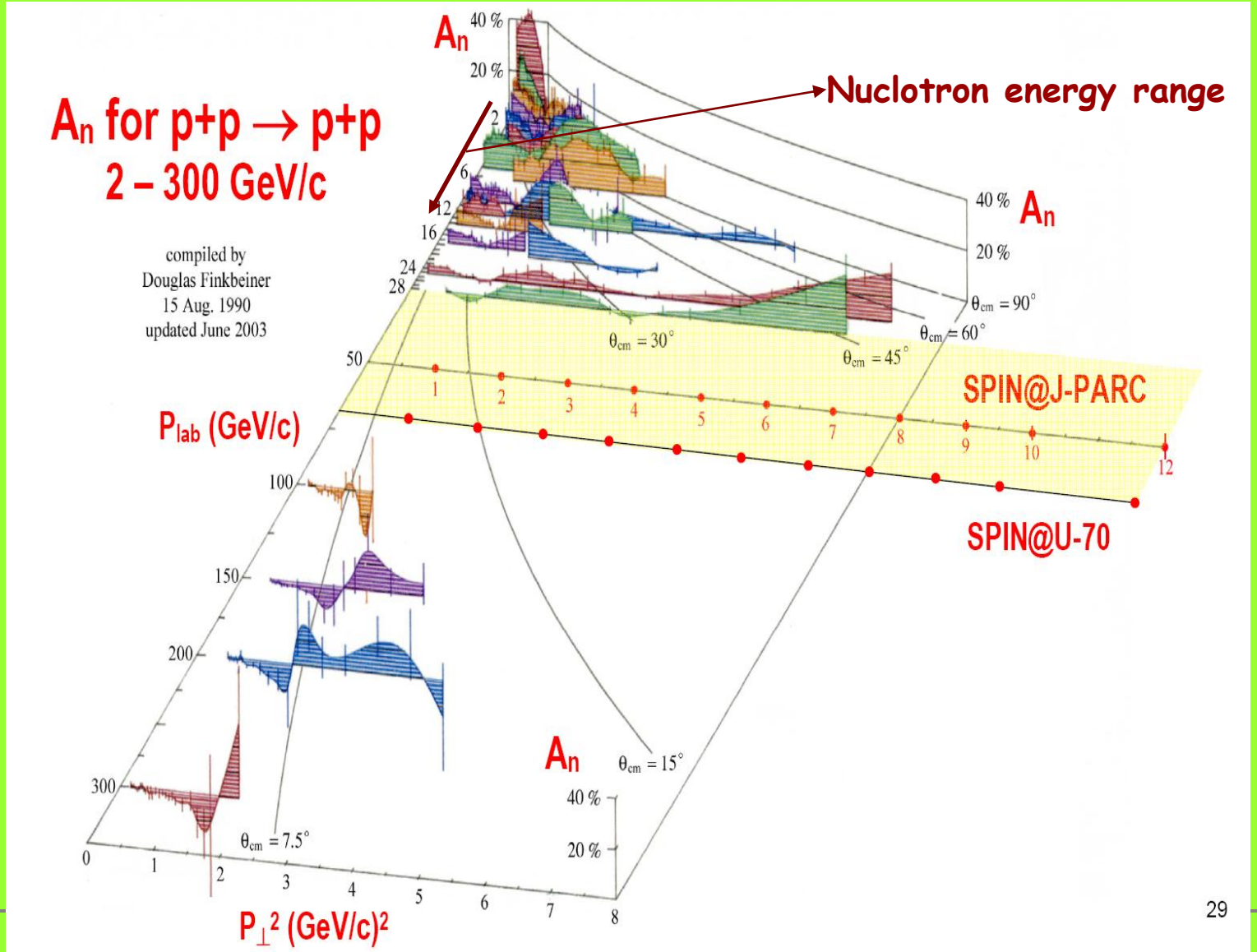
A_n for p+p → p+p
2 – 300 GeV/c
compiled by
Douglas Finkbeiner
15 Aug. 1990
updated June 2003
Nuclotron energy range
A_n
40 %
20 %
$\theta_{cm} = 90°$
$\theta_{cm} = 60°$
$\theta_{cm} = 45°$
$\theta_{cm} = 30°$
$\theta_{cm} = 15°$
$\theta_{cm} = 7.5°$
P_{lab} (GeV/c)
$P_\perp^2$ (GeV/c)²
SPIN@J-PARC
SPIN@U-70
29

PHYSICAL REVIEW D VOLUME 23, NUMBER 3 1 FEBRUARY 1981

Energy dependence of spin-spin effects in p-p elastic scattering at 90°$_{c.m.}$

E. A. Crosbie, L. G. Ratner, and P. F. Schultz
Argonne National Laboratory, Argonne, Illinois 60439

J. R. O'Fallon
Argonne Universities Association, Argonne, Illinois 60439

D. G. Crabb, R. C. Fernow,* P. H. Hansen,† A. D. Krisch, A. J. Salthouse,‡ B. Sandler,§ T. Shima, and K. M. Terwilliger
Randall Laboratory of Physics, The University of Michigan, Ann Arbor, Michigan 48109

N. L. Karmakar
University of Kiel, Kiel, Germany

S. L. Linn‖ and A. Perlmutter
Department of Physics and Center for Theoretical Studies, The University of Miami, Coral Gables, Florida 33124

P. Kyberd
Nuclear Physics Laboratory, Oxford University, Oxford, England
(Received 31 March 1980)

The energy dependence of the spin-parallel and spin-antiparallel cross sections for $p_\uparrow + p_\uparrow \to p + p$ at 90°$_{c.m.}$ was measured for beam momenta between 6 and 12.75 GeV/c. The ratio $(d\sigma/dt)_{\text{parallel}}:(d\sigma/dt)_{\text{antiparallel}}$ at 90° is about 1.2 up to 8 GeV/c and then increases rapidly to a value of almost 4 near 11 GeV/c. Our data indicate that this ratio may depend only on the variable $P_\perp{}^2$, and suggests that the ratio may reach a limiting value of about 4 for large $P_\perp{}^2$.

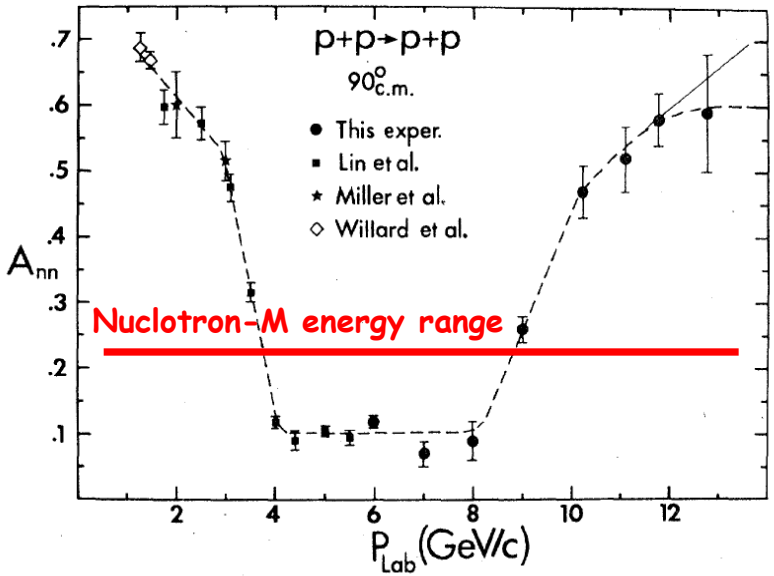

FIG. 2. Plot of the spin-spin correlation parameter A_{nn} for $p+p \to p+p$ at 90°$_{c.m.}$ as a function of incident beam momentum. The dashed and solid lines are hand-drawn possible fits.

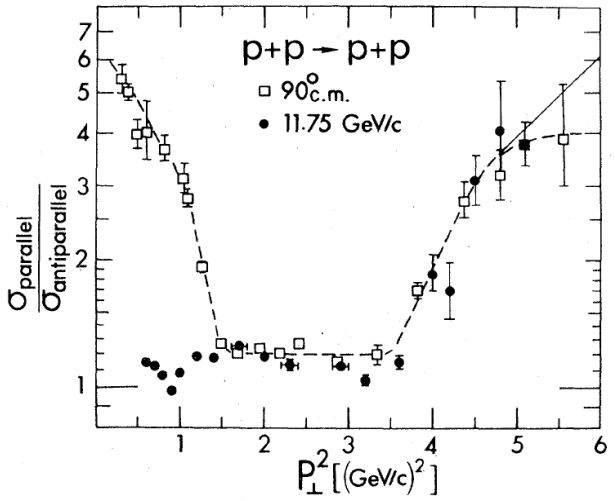

FIG. 3. Plot of the ratio of the spin-parallel to spin-antiparallel differential cross sections, as a function of $P_\perp{}^2$, for p-p elastic scattering. The squares are the fixed-angle data at 90°$_{c.m.}$, with the incident energy varied. The circles are data (Refs. 5, 11) with the momentum held fixed at 11.75 GeV/c while the scattering angle is varied. The dashed and solid lines are hand-drawn possible fits to the 90°$_{c.m.}$ data.

p_T~2 GeV/c anomaly

VOLUME 60, NUMBER 19 PHYSICAL REVIEW LETTERS 9 MAY 1988

Spin Correlations, QCD Color Transparency, and Heavy-Quark Thresholds in Proton-Proton Scattering

Stanley J. Brodsky and Guy F. de Teramond
Stanford Linear Accelerator Center, Stanford University, Stanford, California 94305
(Received 14 January 1988)

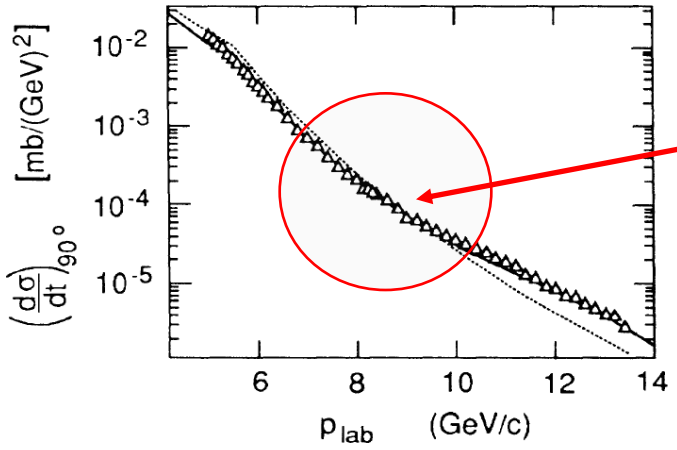

$p_T \sim 2$ GeV/c

FIG. 1. Prediction (solid curve) for $d\sigma/dt$ compared with the data of Akerlof *et al.* (Ref. 16). The dotted line is the background PQCD prediction.

[16]K. Abe *et al.*, Phys. Rev. D **12**, 1 (1975), and references therein. The high-energy data for $d\sigma/dt$ at $\theta_{c.m.} = \pi/2$ are from C. W. Akerlof *et al.*, Phys. Rev. **159**, 1138 (1967); G. Cocconi *et al.*, Phys. Rev. Lett. **11**, 499 (1963); J. V. Allaby *et al.*, Phys. Lett. **23**, 389 (1966).

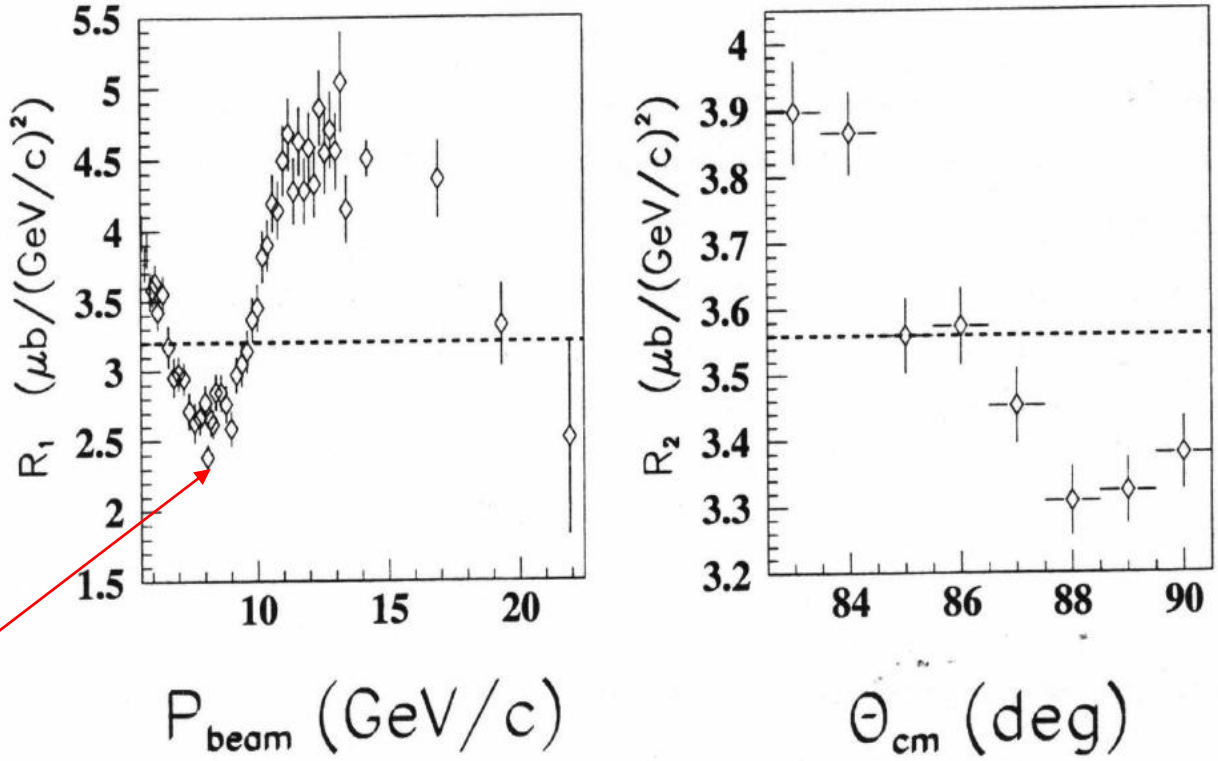

Figure 1.2: Scaled $pp \to pp$ differential cross sections. The dashed lines represent perfect scaling. Their vertical position is arbitrary. **Left** - $R_1 = ((\frac{s}{s_0})^{10} \frac{d\sigma}{dt}(pp))^{-1}$ ($s_0 = 13\ GeV^2$) at $\theta_{cm} = 90^0$ versus incoming momentum. Data are from Ref. [19]. **Right** - $R_2 = (1 - \cos^2\theta_{cm})^{4\gamma} \frac{d\sigma}{dt}(pp)$ ($\gamma = 1.6$) at $p_{lab} = 5.9$ GeV/c versus θ_{cm}. Data are from Ref. [17].

PHYSICAL REVIEW D VOLUME 23, NUMBER 3 1 FEBRUARY 1981

Energy dependence of spin-spin effects in p-p elastic scattering at 90°$_{c.m.}$

E. A. Crosbie, L. G. Ratner, and P. F. Schultz
Argonne National Laboratory, Argonne, Illinois 60439

J. R. O'Fallon
Argonne Universities Association, Argonne, Illinois 60439

D. G. Crabb, R. C. Fernow,* P. H. Hansen,† A. D. Krisch, A. J. Salthouse,‡ B. Sandler,§ T. Shima, and K. M. Terwilliger
Randall Laboratory of Physics, The University of Michigan, Ann Arbor, Michigan 48109

N. L. Karmakar
University of Kiel, Kiel, Germany

S. L. Linn‖ and A. Perlmutter
Department of Physics and Center for Theoretical Studies, The University of Miami, Coral Gables, Florida 33124

P. Kyberd
Nuclear Physics Laboratory, Oxford University, Oxford, England
(Received 31 March 1980)

The energy dependence of the spin-parallel and spin-antiparallel cross sections for $p_\uparrow + p_\uparrow \to p + p$ at 90°$_{c.m.}$ was measured for beam momenta between 6 and 12.75 GeV/c. The ratio $(d\sigma/dt)_{\text{parallel}}:(d\sigma/dt)_{\text{antiparallel}}$ at 90° is about 1.2 up to 8 GeV/c and then increases rapidly to a value of almost 4 near 11 GeV/c. Our data indicate that this ratio may depend only on the variable $P_\perp{}^2$, and suggests that the ratio may reach a limiting value of about 4 for large $P_\perp{}^2$.

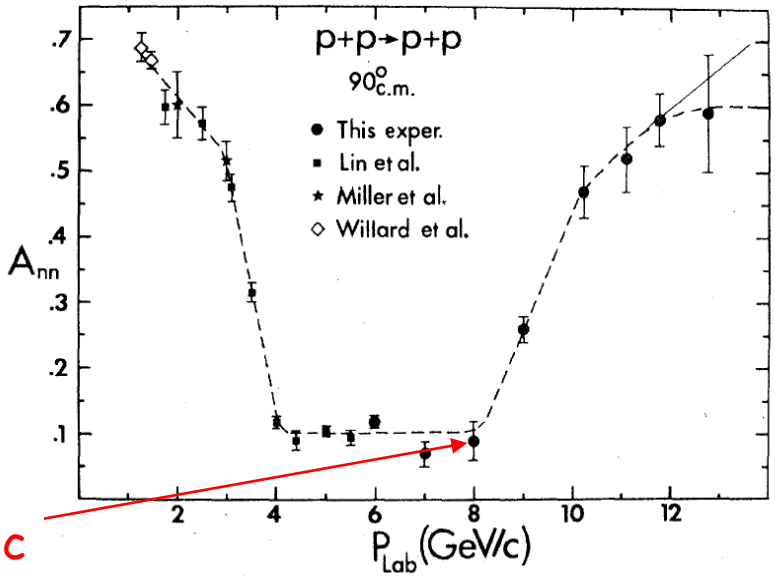

8 GeV/c

FIG. 2. Plot of the spin-spin correlation parameter A_{nn} for $p+p \to p+p$ at 90°$_{c.m.}$ as a function of incident beam momentum. The dashed and solid lines are hand-drawn possible fits.

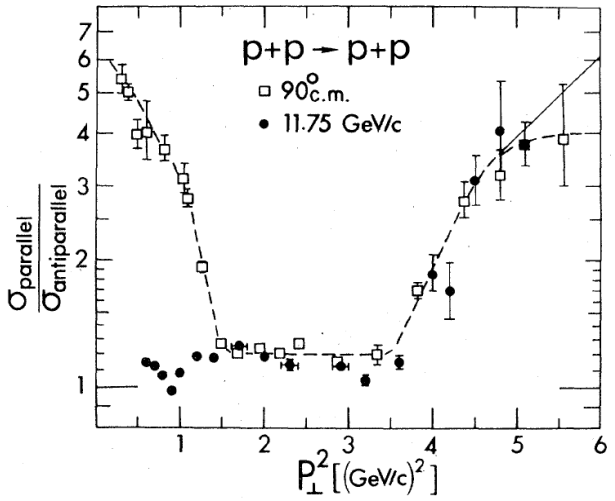

FIG. 3. Plot of the ratio of the spin-parallel to spin-antiparallel differential cross sections, as a function of $P_\perp{}^2$, for p-p elastic scattering. The squares are the fixed-angle data at 90°$_{c.m.}$, with the incident energy varied. The circles are data (Refs. 5, 11) with the momentum held fixed at 11.75 GeV/c while the scattering angle is varied. The dashed and solid lines are hand-drawn possible fits to the 90°$_{c.m.}$ data.

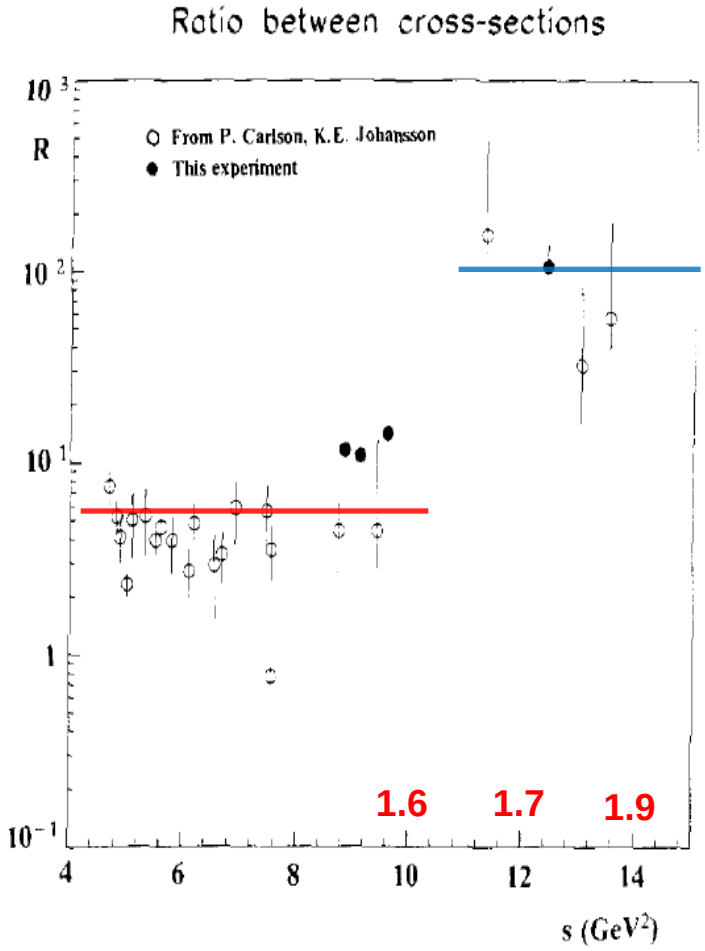

Fig. 4. The ratio between pp and $p\bar{p}$ elastic cross sections at 90° as function of s. The figure is taken from ref. [13] with our data points (shaded circles) added. The pp data used for calculating these ratios for our data points are from ref. [6].

$$\frac{\sigma(pp \to pp)}{\sigma(\bar{p}p \to \bar{p}p)}(90^0\, c.m.)$$

Volume 225, number 3 PHYSICS LETTERS B 20 July 1989

PRECISION MEASUREMENTS OF THE ANTIPROTON–PROTON ELASTIC SCATTERING CROSS SECTION AT 90° IN THE INCIDENT MOMENTUM RANGE BETWEEN 3.5 GeV/c AND 5.7 GeV/c

R-704 Collaboration

VOLUME 87, NUMBER 21 PHYSICAL REVIEW LETTERS 19 NOVEMBER 2001

Energy Dependence of Nuclear Transparency in C(p,2p) Scattering

A. Leksanov,[5] J. Alster,[1] G. Asryan,[3,2] Y. Averichev,[8] D. Barton,[3] V. Baturin,[5,4] N. Bukhtoyarova,[3,4] A. Carroll,[3] S. Heppelmann,[5] T. Kawabata,[6] Y. Makdisi,[3] A. Malki,[1] E. Minina,[5] I. Navon,[1] H. Nicholson,[7] A. Ogawa,[5] Yu. Panebratsev,[8] E. Piasetzky,[1] A. Schetkovsky,[5,4] S. Shimanskiy,[8] A. Tang,[9] J. W. Watson,[9] H. Yoshida,[6] and D. Zhalov[5]

[1]*School of Physics and Astronomy, Sackler Faculty of Exact Sciences, Tel Aviv University, Ramat Aviv 69978, Isra*
[2]*Yerevan Physics Institute, Yerevan 375036, Armenia*
[3]*Collider-Accelerator Department, Brookhaven National Laboratory, Upton, New York, 11973*
[4]*Petersburg Nuclear Physics Institute, Gatchina, St. Petersburg 188350, Russia*
[5]*Physics Department, Pennsylvania State University, University Park, Pennsylvania 16801*
[6]*Department of Physics, Kyoto University, Sakyoku, Kyoto, 606-8502, Japan*
[7]*Department of Physics, Mount Holyoke College, South Hadley, Massachusetts 01075*
[8]*J.I.N.R., Dubna, Moscow 141980, Russia*
[9]*Department of Physics, Kent State University, Kent, Ohio 44242*
(Received 20 April 2001; published 6 November 2001)

The transparency of carbon for $(p, 2p)$ quasielastic events was measured at beam momenta ranging from 5.9 to 14.5 GeV/c at 90° c.m. The four-momentum transfer squared (Q^2) ranged from 4.7 to 12.7 (GeV/c)^2. We present the observed beam momentum dependence of the ratio of the carbon to hydrogen cross sections. We also apply a model for the nuclear momentum distribution of carbon to obtain the nuclear transparency. We find a sharp rise in transparency as the beam momentum is increased to 9 GeV/c and a reduction to approximately the Glauber level at higher energies.

$$T_{\mathrm{CH}} = T \int d\alpha \int d^2\vec{P}_{FT}\, n(\alpha, \vec{P}_{FT}) \frac{(\frac{d\sigma}{dt})_{pp}(s(\alpha))}{(\frac{d\sigma}{dt})_{pp}(s_0)}$$

$$\alpha \equiv A \frac{(E_F - P_{Fz})}{M_A} \simeq 1 - \frac{P_{Fz}}{m_p}$$

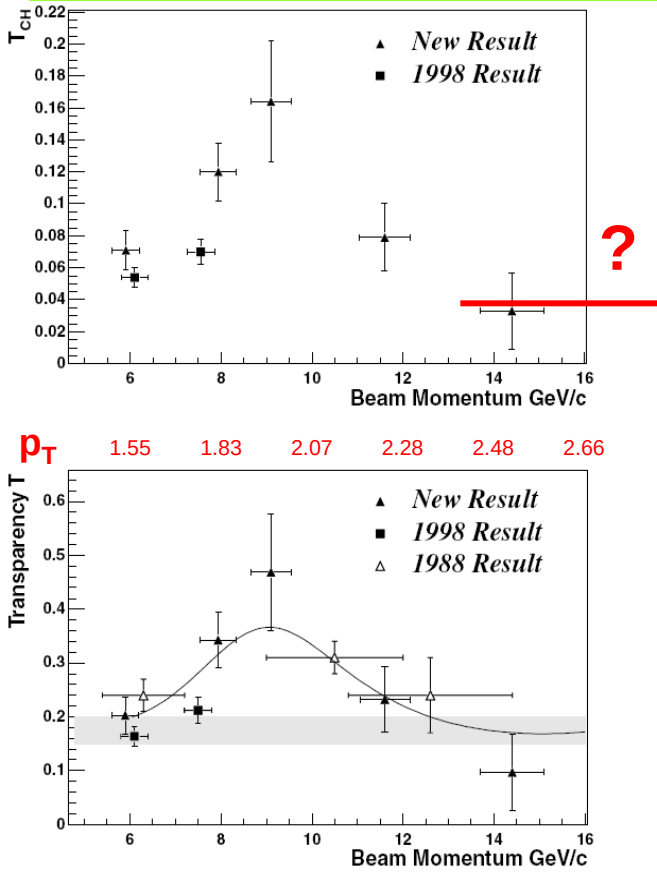

FIG. 2. Top: The transparency ratio T_{CH} as a function of the beam momentum for both the present result and two points from the 1998 publication [3]. Bottom: The transparency T versus beam momentum. The vertical errors shown here are all statistical errors, which dominate for these measurements. The horizontal errors reflect the α bin used. The shaded band represents the Glauber calculation for carbon [9]. The solid curve shows the shape R^{-1} as defined in the text. The 1998 data cover the c.m. angular region from 86°–90°. For the new data, a similar angular region is covered as is discussed in the text. The 1988 data cover 81°–90° c.m.

high p_t suppression seen by all experiments

R_{AA}=yield(AuAu)/N_{coll} yield(pp)

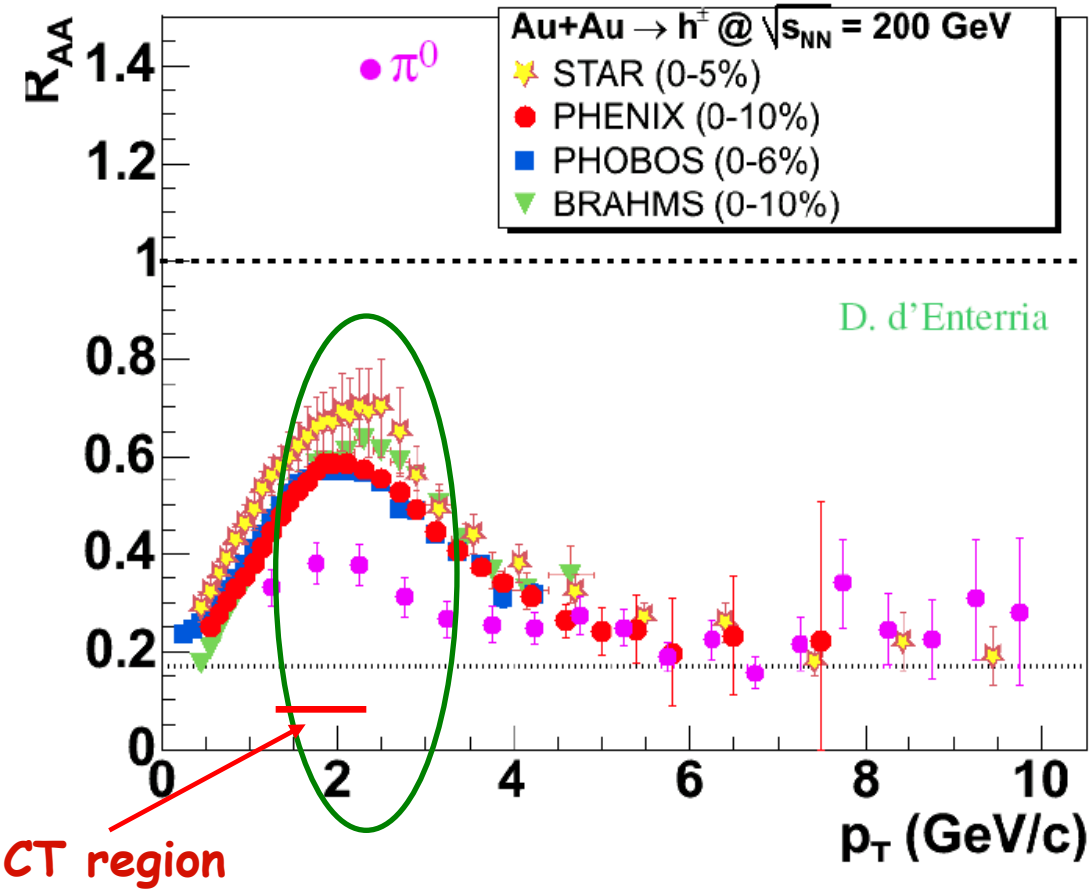

- all expts. see large suppression in AuAu
- π^0 lower than $h^{\pm}$
- no suppression in dAu rather Cronin enhancement → medium effect, not incoming partons

→ reasonable agreement between 4 experiments

ISSN 1063-7788, Physics of Atomic Nuclei, 2009, Vol. 72, No. 12, pp. 1971–1981. © Pleiades Publishing, Ltd., 2009.
Original Russian Text © V.S. Pantuev, 2009, published in Yadernaya Fizika, 2009, Vol. 72, No. 12, pp. 2035–2045.

NUCLEI
Experiment

Recent Results from the Relativistic Heavy Ion Collider (RHIC)*

V. S. Pantuev**

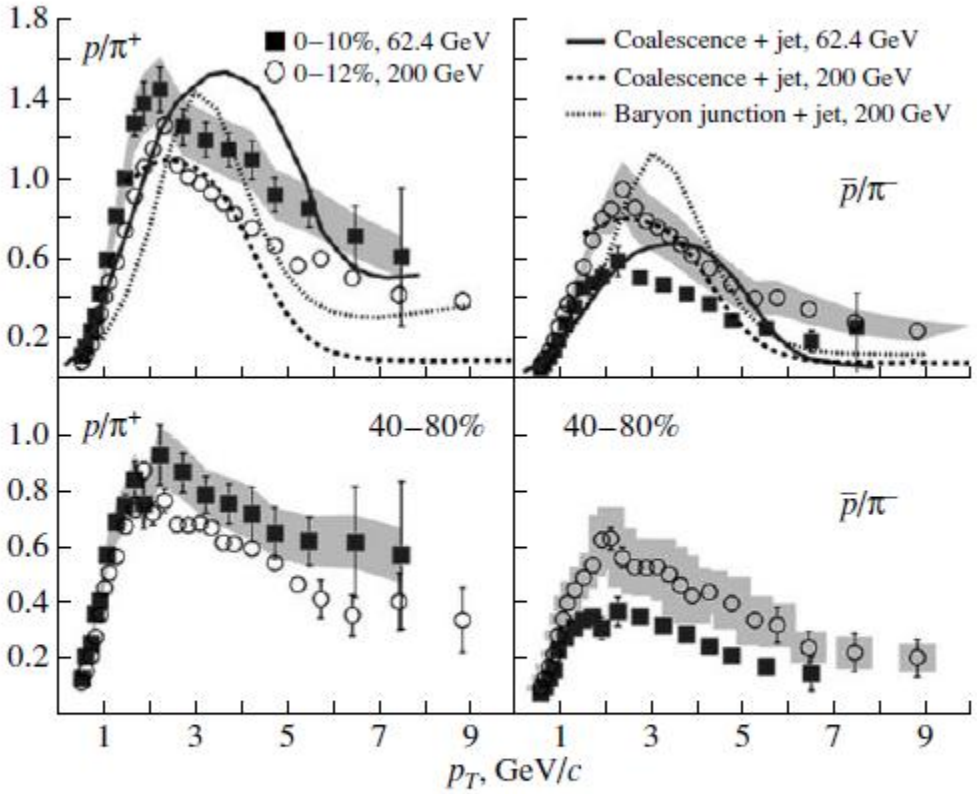

Fig. 3. [10] Ratio of the cross sections for the production of protons and charged pions as a function of the transverse momentum for various degrees of centrality and two beam energies of 62.4 and 200 GeV: (points) results of the STAR experiment and (curves) results of model calculations.

π^0 at $\sqrt{s}$=62 and 500 GeV:

Unpolarized cross section

√s=62 GeV: PRD79, 012003 (2009)

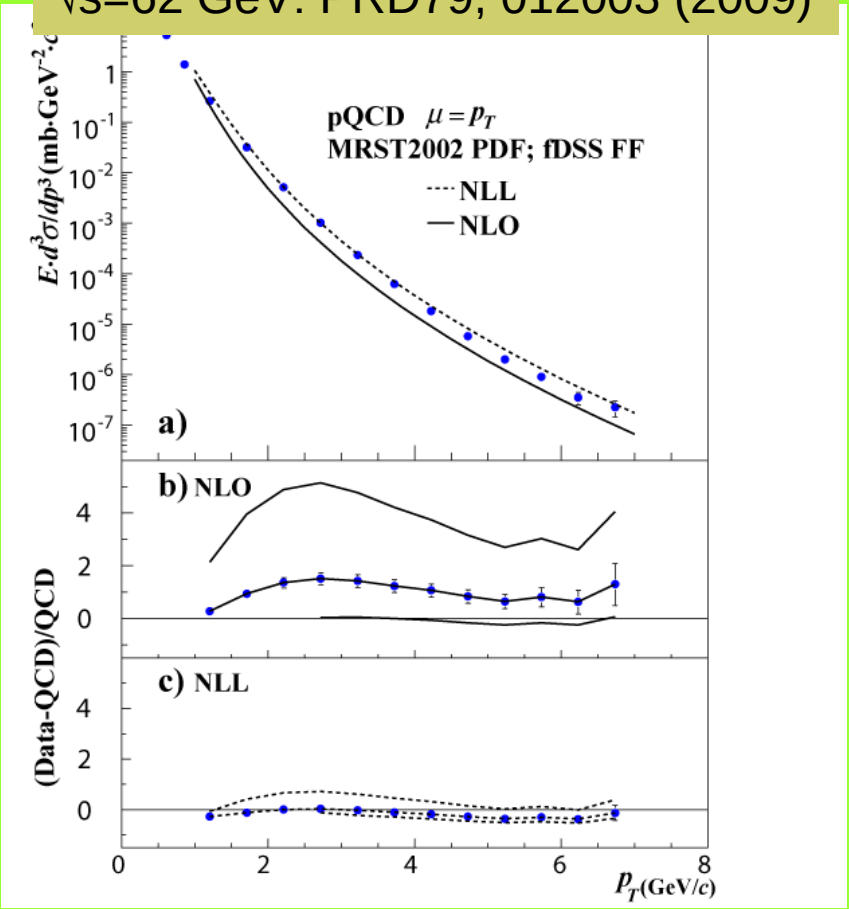

√s=500 GeV: PHENIX Preliminary

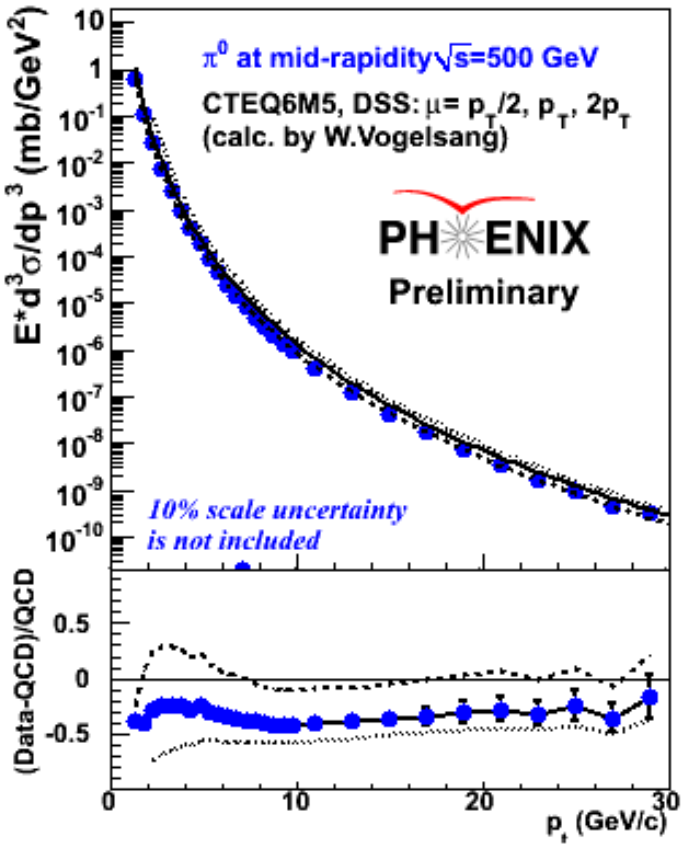

May need inclusion of NLL to NLO

Data below NLO at $\mu = p_T$ by (30±15)%

From soft to hard

PRD76, 051106 (2007)

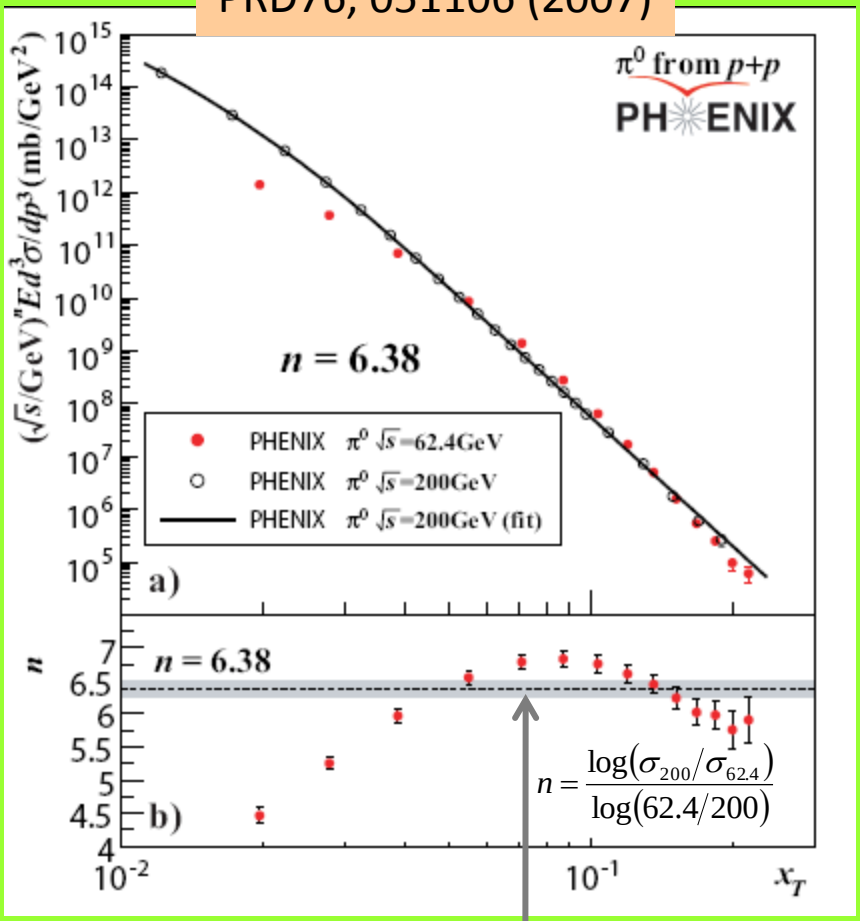

2 GeV/c at √s=62 GeV

x_T scaling:

$$E\frac{d^3\sigma}{dp^3} = \frac{1}{\sqrt{s}^n} G(x_T)$$

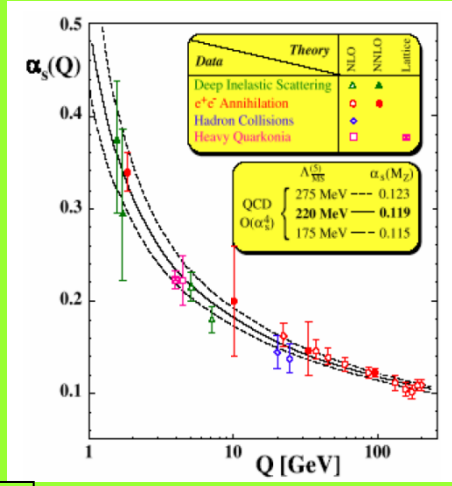

Running $\alpha(Q^2)$
Evolution of PDF and FF
Higher order effects
Etc.

→ $n=n(x_T,\sqrt{s})$

Soft region: $n(x_T)$ increase with x_T
If $\sigma \sim \exp(-\alpha p_T)$
Hard region: $n(x_T)$ decrease with x_T
Stronger scale breaking at lower p_T

$p_T \sim 2$ GeV/c – transition from soft to hard scale?

What "new" we can propose?

We need more complete investigation in the range of maximal p_T in semi-exclusive and exclusive experiments that's why will need new experimental setups for comprehension of the nature of the cumulative processes and CT.

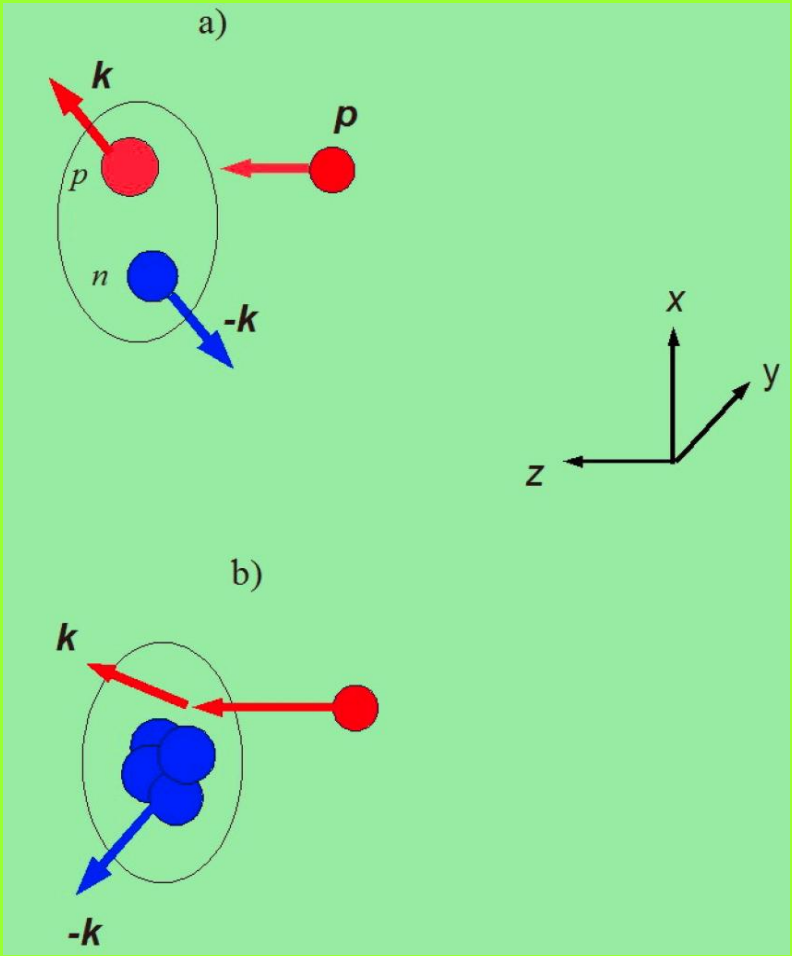

How its can be done?

PNPI (Gatchina) spectrometer 2008
(E < 2GeV proton beams)

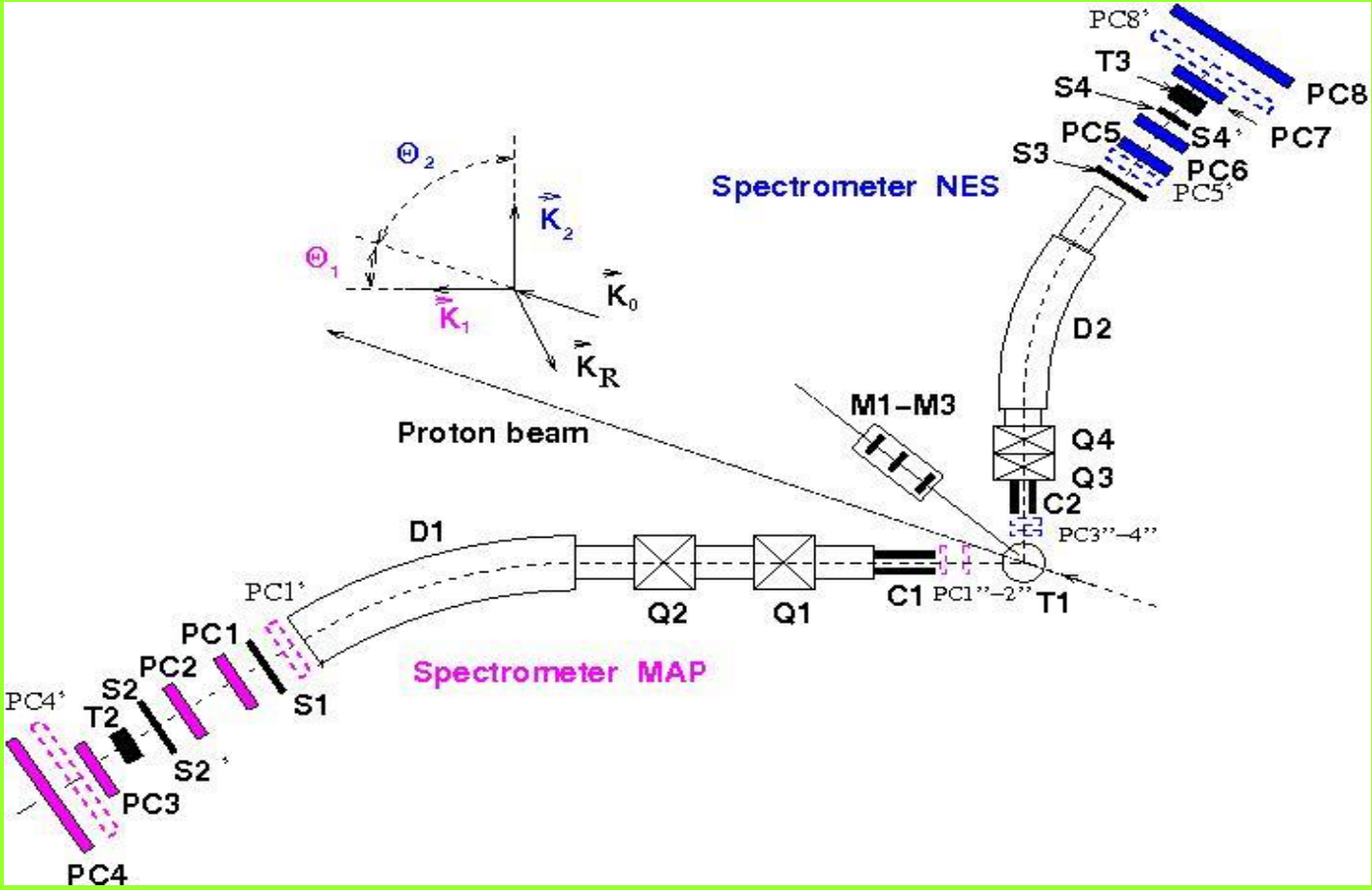

MARUSYA (JINR)
(4.5 GeV/u > E > 0.5 GeV/u)

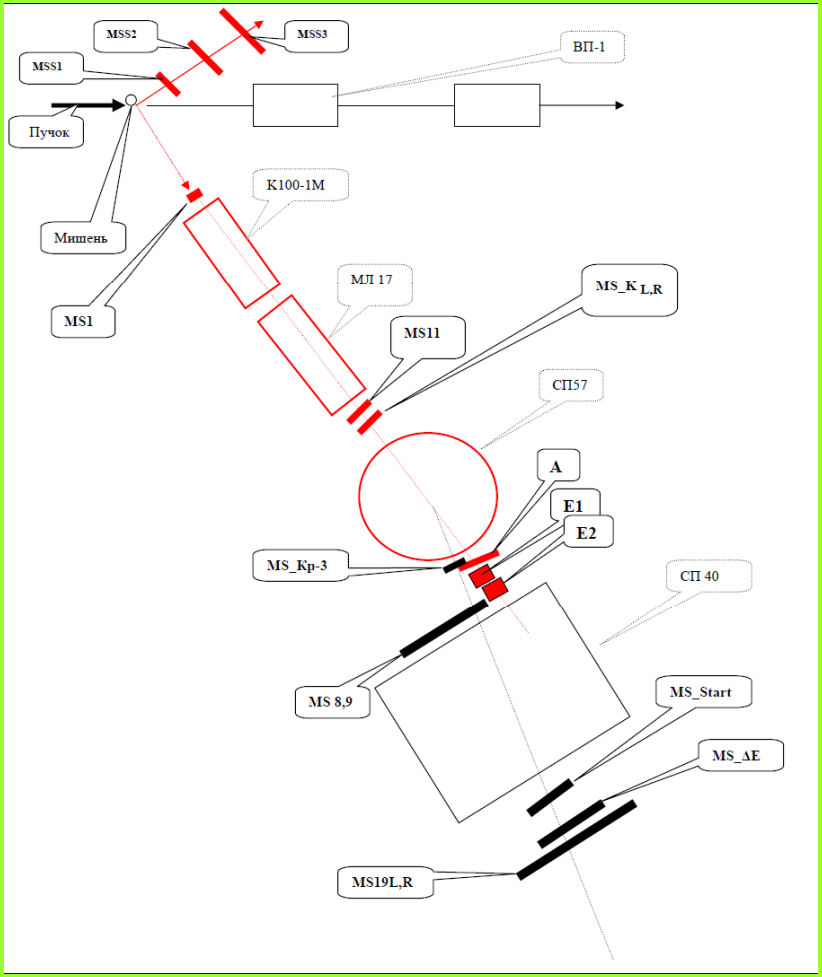

STATE RESEARCH CENTER OF RUSSIA
INSTITUTE FOR HIGH ENERGY PHYSICS

LAYOUT OF IHEP EXPERIMENTAL AREA

E=70 GeV,
I=1.7•10^{13} ppp
Beams of π, K, p, e, ν

- **Fast extraction**
- **Slow extraction**
- **Extraction by crystal**
- **Internal targets**

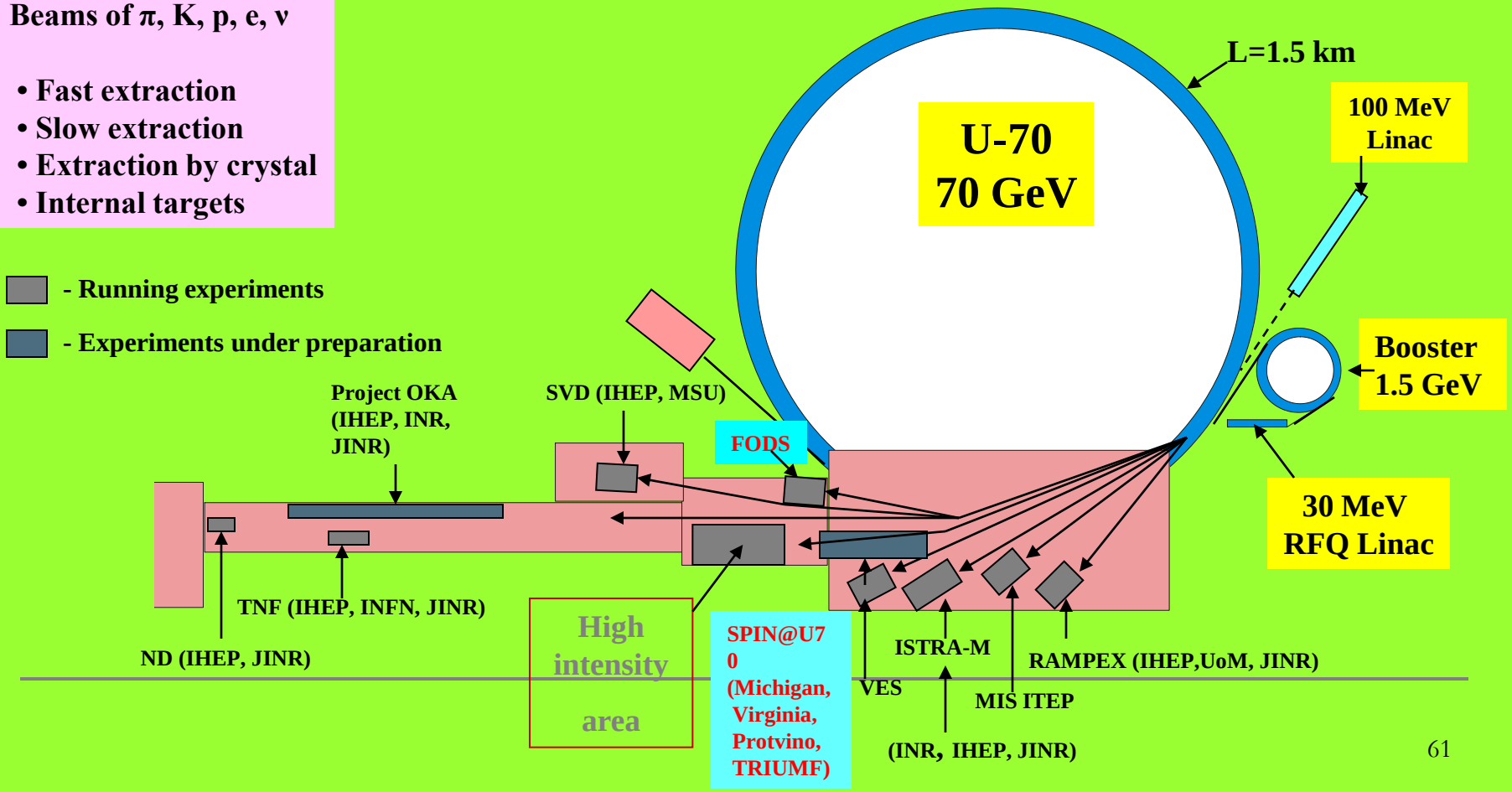

FODS
(proton energy 20-50 GeV and nuclear beams up to 30 GeV/u)

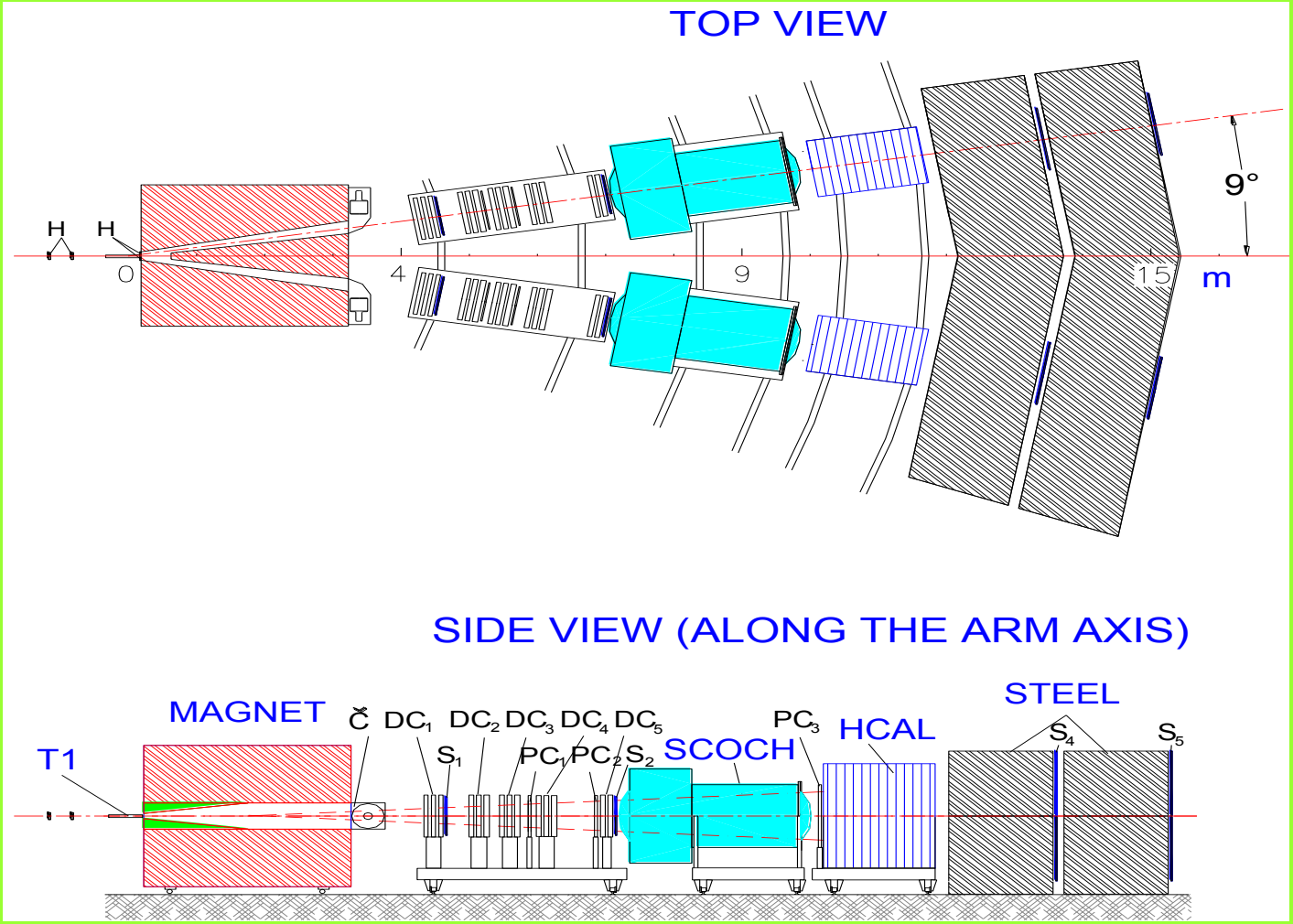

FODS 2010 upgrade

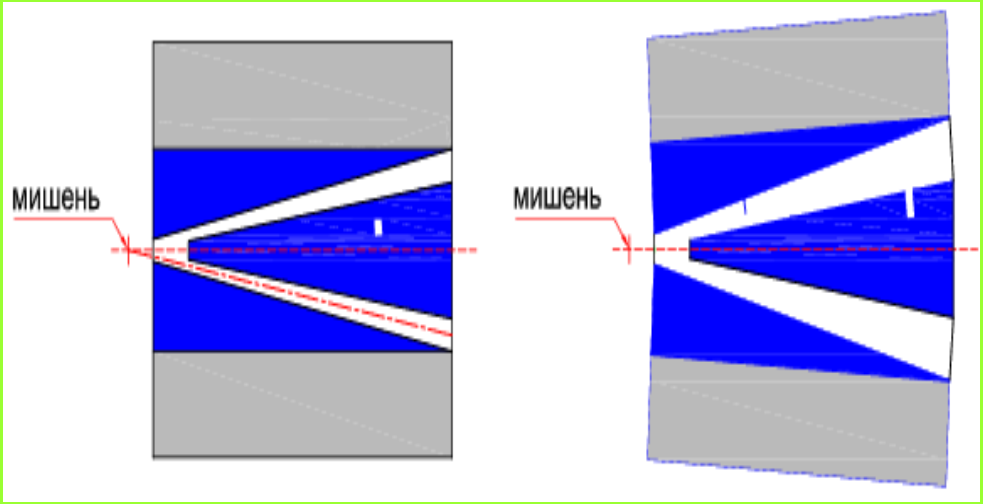

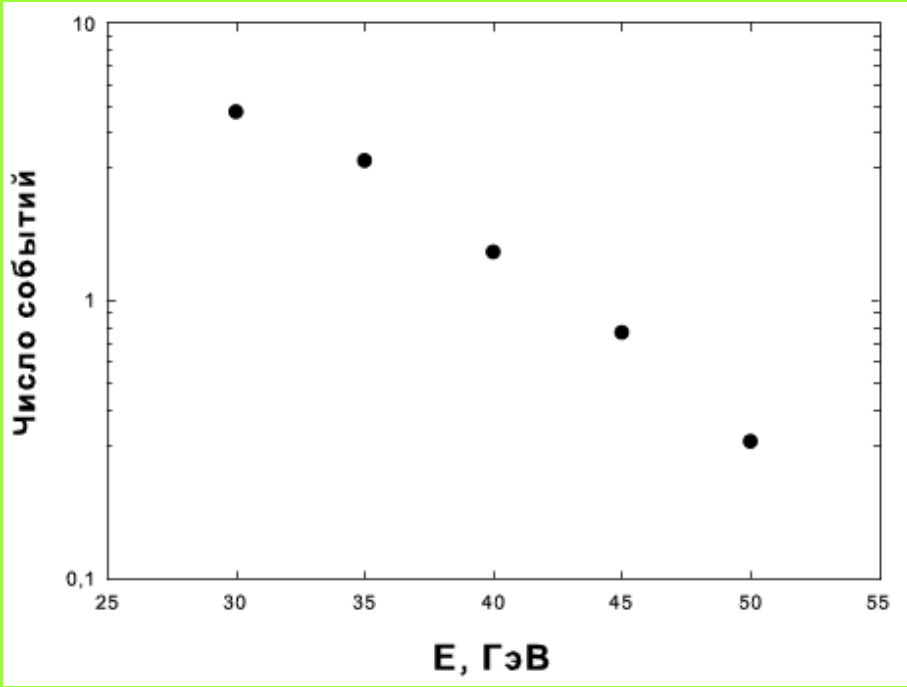

The event rate per day for ^{2}H target (elastic pp at 90^{0} c.m.s.)

SPIN@U70
(proton energy 20-50 GeV)

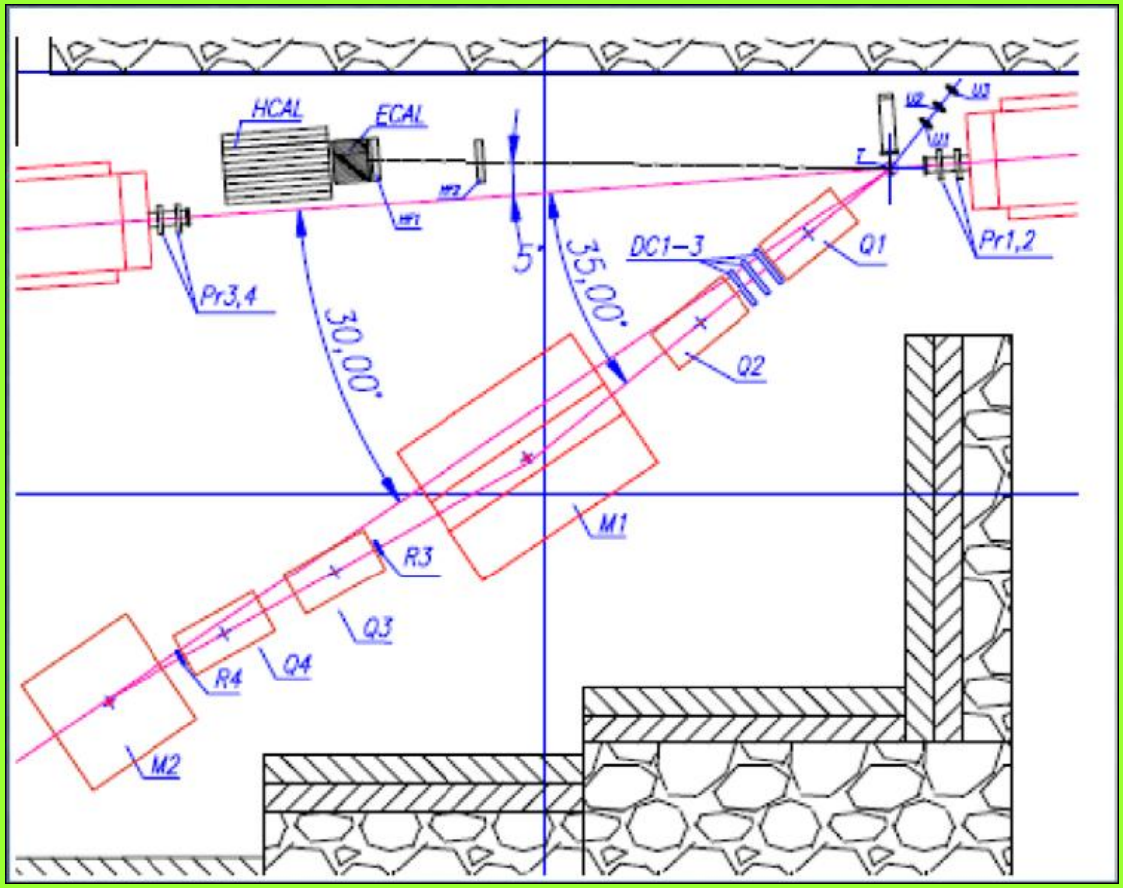

The PANDA Detector (antiproton beams 1-15 GeV)

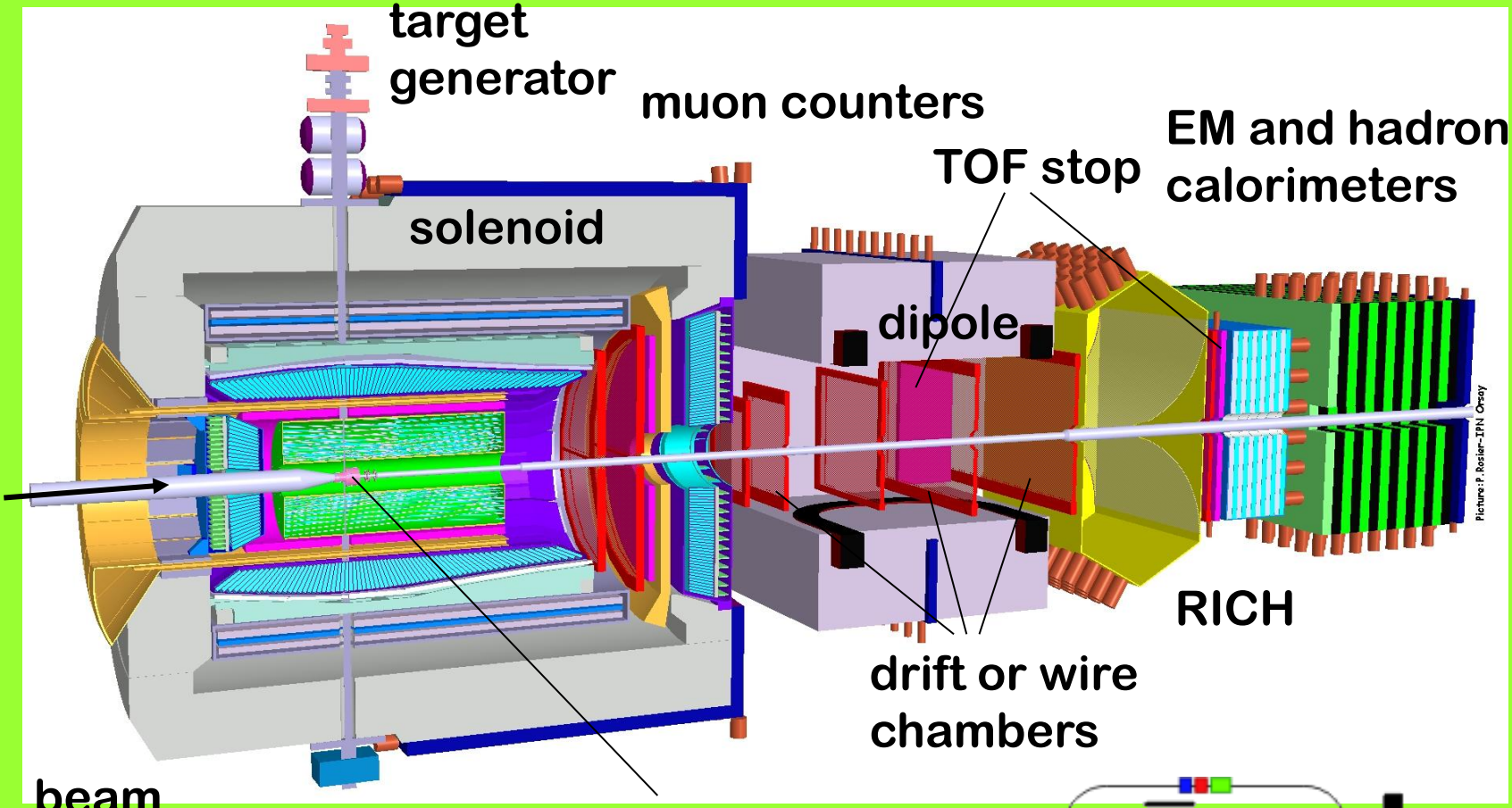

2.2. High p_T $p\bar{p}$ collisions and deep inelastic nuclear reactions with PANDA (S.S.Shimanskiy)

PANDA experiment provides an opportunity to study the properties of the color high density nuclear matter (CHDNM), which differs from Quark Gluon Plasma (QGP) state [1]. To detect the CHDNM one has to study the *p A* - collisions in kinematical region beyond the kinematical limits for interacting with free nucleons (named as cumulative processes).

We propose [7] to perform the measurement of three deep inelastic antiproton-nuclei processes (DINP):

- The first one is a DINP $\bar{p} + A \to \bar{p} + < mN >$, where m is an average number of nucleons. The final state antiproton must have $x_T = \frac{2p_T}{\sqrt{s}} \sim 1$, where $s = (p_{\bar{p}} + p_N)^2$. The aim is to see the dependence on the cumulative number X. SRC mechanism predicts <m> ≈ 1 and no dependence on X.
- The second process is the subthreshold J/Ψ (and D-mesons) production: $\bar{p} + A \to J/\Psi + X \to \mu^+\mu^- + X$ at $E_{beam} \geq 2-3$ GeV. Dimuon pair must have $E^{\mu\mu} \geq 1.5$ GeV. The aim is to measure the cross section of this process which can be greater than the subthreshold cross section of antiproton production $p + A \to \bar{p} + X$ [8] which is already measured [4]. There is a prediction that the case $\sigma(\bar{p} + A \to J/\Psi + X) > \sigma(p + A \to \bar{p} + X)$ can be treated in favor of "flucton" hypothesis.

Collider experiments at NICA

NICA Collider 2T- 534

The main elements of spin manipulation

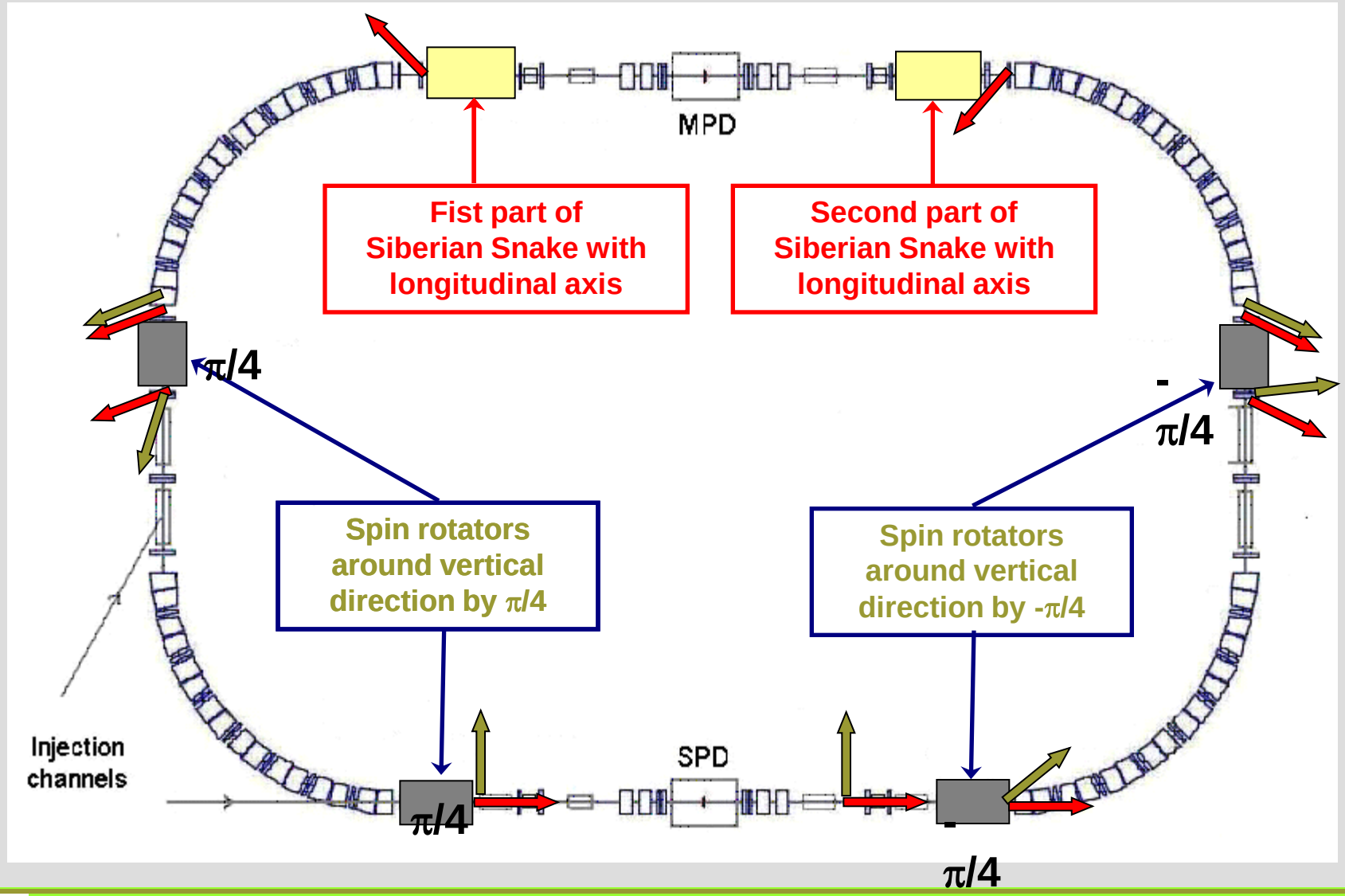

NICA Collision place for SPIN physics (deuteron and other beams)

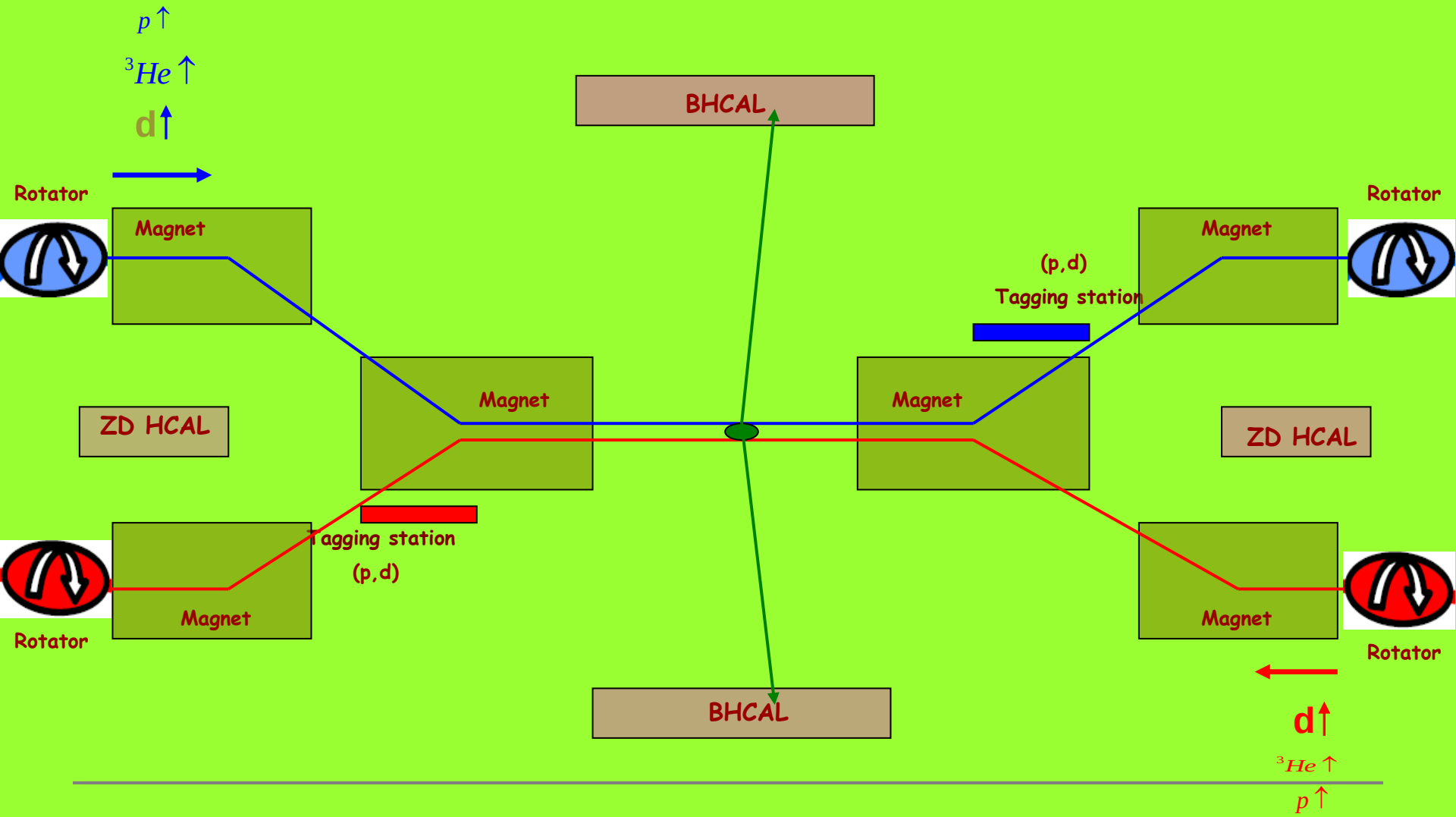

With polarized ion beams we have real possibility to resolve many problems as are:

-"Spin crisis" of 70's ($p\vec{}p\vec{}$, $p\vec{}n\vec{}$, $n\vec{}n\vec{}$);

- Color transparence ($p\vec{}A$, $p\vec{}^{3}He(d)\vec{}$);

-Cumulative (subthreshold) particle production – to discovery the new state of nuclear Matter …

"NEW"- exclusive reactions $N\uparrow + N\uparrow \to BB + MM(\overline{M})$

where B – baryons N, Λ, Δ^{B+M} …,

M – mesons or leptons

(diquarks, qq -vertex…).

For example

$$p\uparrow + p\uparrow \rightarrow p + p + \pi^0\pi^0(\pi^+\pi^-)$$

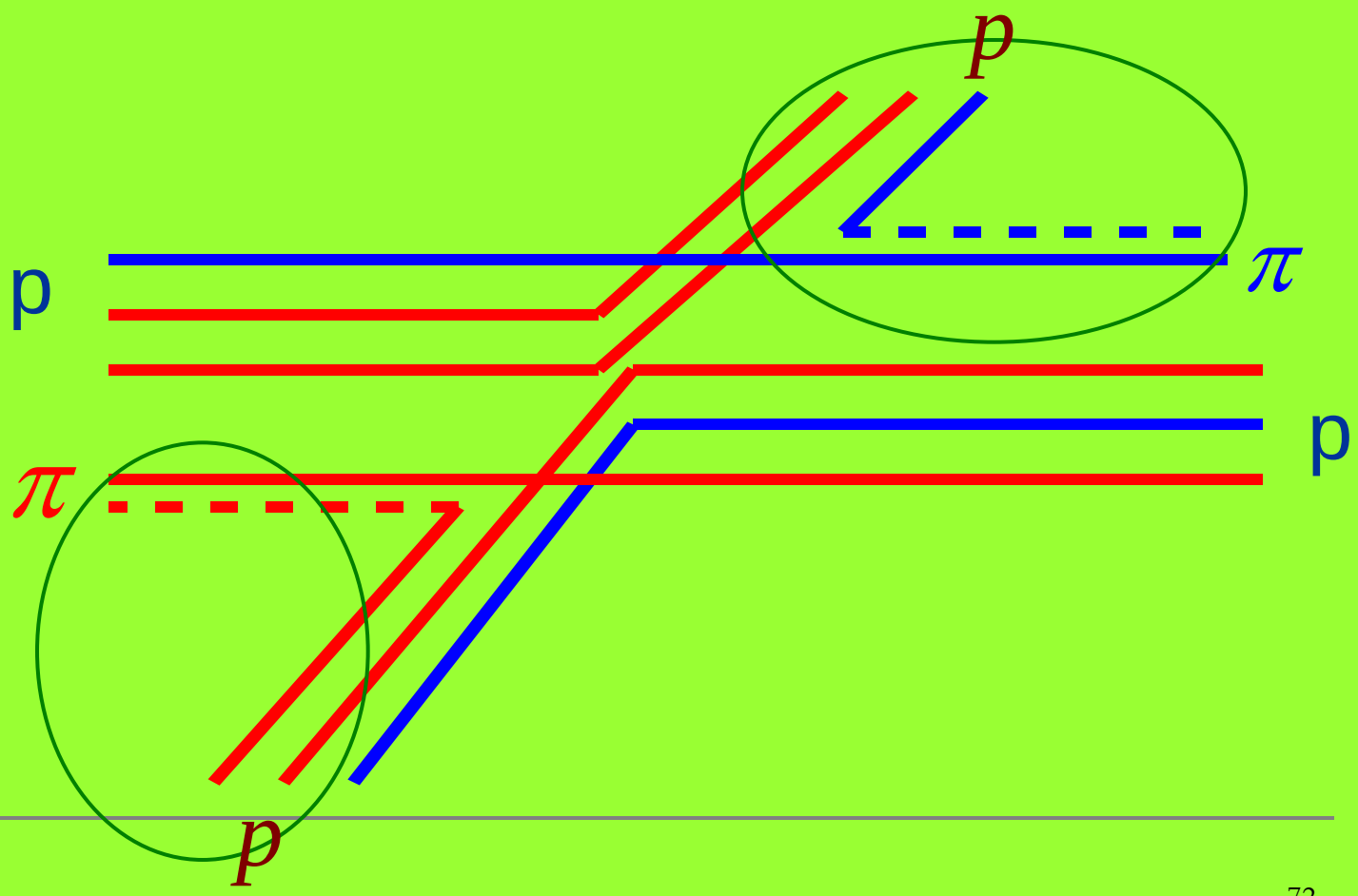

END

H_2O Phase Diagram